UPPSALA
UNIVERSITET

Digital Comprehensive Summaries of Uppsala Dissertations from the Faculty of Science and Technology 2142

Oversampled radial basis function methods for solving partial differential equations

IGOR TOMINEC

ACTA
UNIVERSITATIS
UPSALIENSIS
UPPSALA
2022

ISSN 1651-6214
ISBN 978-91-513-1486-0
URN urn:nbn:se:uu:diva-472096

Dissertation presented at Uppsala University to be publicly examined in Heinz-Otto Kreiss lecture hall, Ångströmlaboratoriet, Lägerhyddsvägen 1, Uppsala, Tuesday, 31 May 2022 at 13:15 for the degree of Doctor of Philosophy. The examination will be conducted in English. Faculty examiner: Professor Bengt Fornberg (University of Colorado Boulder, USA).

Abstract
Tominec, I. 2022. Oversampled radial basis function methods for solving partial differential equations. *Digital Comprehensive Summaries of Uppsala Dissertations from the Faculty of Science and Technology* 2142. 48 pp. Uppsala: Acta Universitatis Upsaliensis.
ISBN 978-91-513-1486-0.

Partial differential equations (PDEs) describe complex real-world phenomena such as weather dynamics, object deformations, financial trading prices, and fluid-structure interaction. The solutions of PDEs are commonly used to enhance the understanding of these phenomena and also as leverage to make technological improvements to consumer products. In the present thesis, we develop numerical methods for solving PDEs using computers. The focus is on radial basis function (RBF) methods that are appreciated for their high-order accuracy and ease of implementation in higher dimensions, but can sometimes face numerical stability challenges. To circumvent the stability issues, we use an oversampled approach to discretize PDEs as opposed to the more commonly used collocated approach. Throughout the thesis, we mainly use the RBF-generated finite difference (RBF-FD) method, but we also use the RBF partition of unity method (RBF-PUM) and Kansa's global RBF method in one part of the thesis. The first two methods are local in the sense that the underlying discretization matrices are sparse, while the third method is global, leading to dense discretization matrices. In Paper I we improve the stability properties of the RBF-FD method through an oversampling approach when solving an elliptic model problem with derivative-type boundary conditions, and provide a theoretical analysis. In Paper II we develop an unfitted RBF-FD method and by that simplify the handling of complex computational domains by relaxing the requirement that the set of nodes has to conform to the boundary of the domain. We make the first steps toward a simulation of the thoracic diaphragm in Paper III, where we use an unfitted RBF-FD method to solve a linear elastic PDE and employ data smoothing to leverage high-order convergence of the numerical solution. In Paper IV we explore the stability properties behind the RBF-FD method, Kansa's method, and RBF-PUM when they are applied to a linear time-dependent hyperbolic PDE. We find that Kansa's method and RBF-PUM can become stable under sufficient oversampling of the system of equations. On the other hand, the insufficient regularity of the numerical solution prevents the RBF-FD method from being stable in time, no matter the oversampling. In Paper V we use the residual viscosity stabilization framework to locally stabilize the Gibbs phenomenon present in the RBF-FD solutions to shock-inducing nonlinear time-dependent conservation laws such as the compressible Euler system of equations.

Keywords: radial basis function, PDE, oversampling, stability, RBF-FD, RBF-PUM, unfitted

Igor Tominec, Department of Information Technology, Division of Scientific Computing, Box 337, Uppsala University, SE-751 05 Uppsala, Sweden.

ISSN 1651-6214
ISBN 978-91-513-1486-0
URN urn:nbn:se:uu:diva-472096 (http://urn.kb.se/resolve?urn=urn:nbn:se:uu:diva-472096)

To Eva and Sever.

List of papers

This thesis is based on the following papers, which are referred to in the text by their Roman numerals.

I I. Tominec, E. Larsson, A. Heryudono. A least squares radial basis function finite difference method with improved stability properties. *SIAM Journal on Scientific Computing, Vol. 43, no 2., February 2021.*

Contributions: The author of the thesis came up with the idea for the method and an initial outline for how to perform the analysis, implemented the methods, performed the numerical experiments, and wrote the manuscript in collaboration with the other authors.

II I. Tominec, E. Breznik. An unfitted RBF-FD method in a least-squares setting for elliptic PDEs on complex geometries. *Journal of Computational Physics, Vol. 436, July 2021.*

Contributions: The author of the thesis initiated the project, implemented the methods in collaboration with the second author, designed and performed the numerical experiments, and wrote the manuscript in collaboration with the second author.

III I. Tominec, P-F. Villard, E. Larsson, V. Bayona, N. Cacciani. An unfitted radial basis function generated finite difference method applied to thoracic diaphragm simulations. *arXiv e-prints: arXiv:2103.03673, March 2021. In revision.*

Contributions: The author of the thesis implemented the methods, performed the numerical experiments involving the radial basis function method, and wrote the manuscript in collaboration with the other authors.

IV I. Tominec, M. Nazarov, E. Larsson. Stability estimates for radial basis function methods applied to time-dependent hyperbolic PDEs. *arXiv e-prints: arXiv:2110.14548, October 2021. Submitted.*

Contributions: The author of the thesis initiated the project, performed the theoretical analysis, implemented the methods, performed the numerical experiments, and wrote the manuscript in collaboration with the other authors.

V I. Tominec, M. Nazarov. Residual viscosity stabilized RBF-FD methods for solving nonlinear conservation laws.
arXiv e-prints: arXiv:2109.07183, September 2021. Submitted.

Contributions: The author of the thesis implemented the methods, performed the numerical experiments, and wrote the manuscript in collaboration with the second author.

Reprints were made with permission from the publishers.

Contents

1. Introduction

Mathematical models can describe natural phenomena. These models represent a relationship between a quantity possible to observe and a quantity that we would like to obtain knowledge about and we cannot make observations on. As a crude example, consider measuring the velocity of a car driving by as time passes, using a device that only displays the car's velocity. Say that we would also like to know the distance the car traveled, at each point in time $t > 0$ from $t = 0$ onwards. To recover the unknown distance function $s(t)$ we first have to find a relation between $s(t)$ and the known velocity function $v(t)$. This relation is called a mathematical model, and is in the present case given by: $v(t) = \partial_t s(t)$, where t is time, and $\partial_t s(t)$ is a very small change of the distance function in time (a derivative in time). This mathematical model is called an ordinary differential equation: "differential" as the equation contains a derivative and an "ordinary" because the involved functions only depend on one variable (time). When a differential equation contains unknown functions that depend on several variables, the equation is called a partial differential equation. Both ordinary and partial differential equations (PDEs) are generally not trivial (and sometimes impossible) to solve by pen and paper, depending on the complexity of the mathematical model. A branch of mathematics called numerical mathematics (or numerical analysis or computational mathematics, or scientific computing) deals with approximations of solutions to differential equations by breaking one differential equation down into many simpler algebraic equations, which a computer knows how to solve. "Many simpler equations" means, for example, a set of millions of simpler equations. Typical mathematical questions are whether the solution to the "many simpler equations" can be uniquely determined and whether such a unique solution gives a good approximation to the exact solution of the differential equation. Another critical question is whether the algorithm to convert a differential equation to "many simpler equations" and then to solve those equations with a computer is feasible to use in terms of the required computational time. A side question is whether the computer implementation requires significant efforts in terms of human labor.

From here on we start using mathematical terminology to provide an introduction to the papers included this thesis. A function $\Phi(y) : \mathbb{R}^d \to \mathbb{R}$, $d = 1, 2, 3, \ldots$, is called *radial* when $\Phi(y) = \Phi(\|y\|_2)$, i.e., when the argument of the function only depends on the distance measured from the origin. Here $\|y\|_2 = \sqrt{y_1^2 + y_2^2 + \ldots + y_d^2}$ is the Euclidean (radial) distance function. These

functions are commonly used for multivariate data approximation (interpolation) or for computing solutions to PDEs. We refer to the functions as radial basis functions (RBFs). RBF methods for solving PDEs are different from the other available methods because they do not require the domain Ω to be split into small geometrical elements. A collection of these elements is called a mesh. Instead, RBF methods work with a set of points scattered throughout Ω. A set of points is in some cases also subdivided into many local point sets, but the local point sets do not have to conform to a predefined geometrical shape. The RBF methods are many times called meshfree (also meshless) methods. They give numerical solutions with high-order convergence when the PDE data is smooth, and are simple to implement on a computer, especially in higher dimensions. A disadvantage of using meshfree methods can be that the approximate solution is prone to different kinds of numerical instabilities when solving PDEs.

The present dissertation focuses on RBF methods to solve PDEs. We provide new insights in terms of the stability properties of the RBF methods. We make method improvements based on these findings and method improvements related to simplifying the handling of complex geometries. We use the improved methods for applications in biomechanics and fluid mechanics. In the following sections of this introduction, we provide an overview of the radial basis function research directions relevant to the context of this thesis.

1.1 Interpolation using radial basis functions with global support

To be able to interpolate a function is an essential step when developing a method for solving PDEs. In paper [32] from 1971, Hardy was the first researcher to use a sequence of radial functions $\Phi_k(y) = \Phi(y - x_k)$, $k = 1,..,N$, to construct a multivariate interpolation problem where the interpolation data $f_k = f(x_k)$ was a topographic surface. Here y is an evaluation point and x_k is the node where Φ_k is centered at. Hardy was looking for a representation of a topographic surface $s(y)$ using an ansatz:

$$s(y) = \sum_{k=1}^{N} c_k \Phi_k(y), \tag{1.1}$$

where c_k, $k = 1,..,N$, were determined by solving the problem:

$$s(x_i) = f_i, \quad i = 1,..,N.$$

Hardy used the multiquadric type of RBFs, $\Phi_k(y) = \sqrt{1 + \varepsilon^2 \|y - x_k\|^2}$, where ε is a so-called shape parameter. The shape parameter decides how flat an RBF is, see Figure 1.1. There exist many different radial basis functions. We

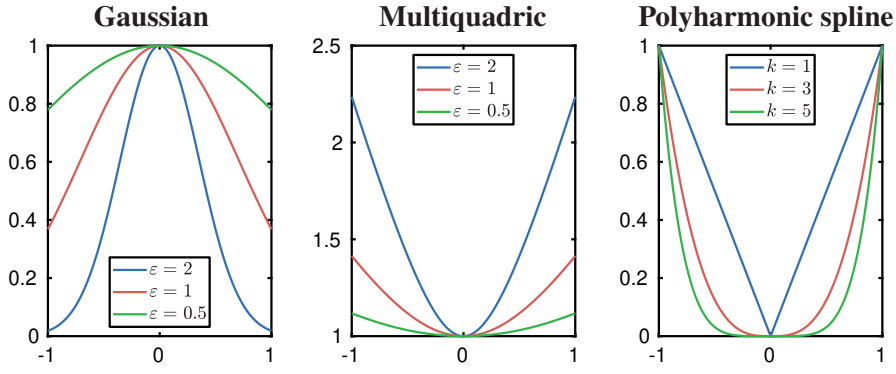

Figure 1.1. Three different types of radial functions in one dimension, centered around the origin.

provide a few of them in the table below. RBFs can be subdivided into two groups. The first group consists of RBFs dependent on a shape parameter ε. The second group consists of RBFs with no dependence on ε.

A few types of radial functions	
Gaussian	$\Phi(y) = e^{-\varepsilon^2 \|y\|_2^2}$
Multiquadric (MQ)	$\Phi(y) = (1+\varepsilon^2 \|y\|_2^2)^{\frac{1}{2}}$
Inverse MQ	$\Phi(y) = (1+\varepsilon^2 \|y\|_2^2)^{-\frac{1}{2}}$
Polyharmonic spline	$\Phi(y) = \|y\|_2^k, \quad k = 1,3,5,\ldots$

In the present thesis we use RBFs that have no dependence on ε.

1.2 An overview of partial differential equation discretizations using radial basis functions

This section provides an overview of the existing RBF discretization methods for solving PDEs. We subdivide those into a group of methods that construct a sequence of cardinal (interpolatory) basis functions with global support and a group of methods that construct the cardinal (interpolatory) basis functions with local support. Another subdivision is the residual minimization framework that is used, such as the collocation approach, the Galerkin approach or an oversampled approach (often referred to as a least-squares approach).

Discretizations of partial differential equations using radial basis functions with global support

An ever-present justification for using RBFs for discretizations of PDEs has been that RBF interpolants are easy to implement and work well for scattered

data approximation in high dimensions. By using RBFs, we are not limited to computing PDE solutions over tensor grid domains, as in the classical finite difference setting or a pseudospectral setting, but it is possible to compute solutions over complex domains discretized by scattered points. A direct competitor have always been the finite element methods, where an argument for RBF methods has been that an engineer is not required to compute a mesh discretizing a complex domain. Instead, it is possible to work only with sets of points scattered throughout the computational domain. Among the justifications are also the ease of implementation of the RBF methods, where two significant contributions add to the simplicity: (i) each basis term of an RBF interpolant is only a translate of the same RBF, where any derivatives of that term are then easy to obtain, while, for example, each term of the multivariate monomial basis takes a different form (for example, a few terms in 2 dimensions are: $1, x, y, xy, x^2, y^2, ..$) which then requires an investment of additional effort when it comes to implementing the basis in higher dimensions and evaluating its derivatives, (ii) typically, RBF methods discretize PDEs by collocating the derivatives at nodes (collocation), avoiding the variational framework, which requires the implementation of quadrature rules in high dimensions.

The beginnings of PDE discretizations using RBFs go back to 1986 when Kansa in [37] used Hardy's multiquadric interpolant [32] to approximate spatial derivatives in a time-dependent PDE hydrodynamics model (coupled density, momentum, pressure, and energy), and then advance the solution in time using a classical explicit Runge-Kutta 4 method. The spatial derivatives were evaluated at node locations without employing any variational principles. Thus, the PDE discretization was of collocation type. A few years later, in 1990, Kansa evaluated the approximation errors of multiquadric interpolation and derivative approximation [38], and also used multiquadrics in a collocation setting to compute solutions to elliptic, parabolic and hyperbolic PDEs [39]. In both papers, he found a good agreement with exact solutions and faster convergence of the approximation error compared with the (low-order) finite difference methods. The method that Kansa used is commonly referred to as Kansa's global RBF method.

Kansa's papers then gave a rise to further usage of the RBF collocation methods, and also to their analysis [27, 28, 16]. The discrete well-posedness of the discretizations made by using RBF collocation methods is still an open question. Instead of using collocation, researchers have, in a few papers, used a variational form through the Galerkin projection [73, 40, 35], where discrete well-posedness and convergence have been proved. However, those methods generally require quadrature algorithms exact for integrating the basis functions that span the approximation space. These algorithms add to the complexity when implementing the algorithm, especially in higher spatial dimensions.

A middle ground between a fully variational projection (employing exact integration) and collocation is the so-called oversampling (also overtesting) approach, where the derivatives in the PDE are discretized pointwise just as

in the collocation case, but the set of these points is larger than the set of nodes that correspond to the unknown nodal values. The result is a rectangular system of equations which is then reformulated into a square system of equations by employing a discrete projection either onto the system's own column space or onto the column space of another matrix. Due to the projection, it is then easier to establish well-posedness results for some PDEs [58, 47, 42, 14]. There is no need to employ quadrature exact for integrating the basis functions that span the approximation space, so the overall algorithm implementation efforts are similar to the collocation case.

The oversampling approach is used to discretize PDEs within the present thesis.

Discretizations of partial differential equations using radial basis functions restricted to local supports

At first, PDE discretizations using RBFs were global, i.e., the radial basis functions had a global support throughout the computational domain. As a consequence, the resulting systems of equations were dense. Computations using dense systems of equations are expensive. In the 2000s two major localization approaches emerged that led to sparse systems of equations: the radial basis function generated finite difference (RBF-FD) method due to Tolstykh [66, 21] and the radial basis function partition of unity method (RBF-PUM) due to Lazzaro and Montefusco in [46] and due to Wendland in [74]. The partition of unity method was initially introduced by Babuška and Melenk [2]. Both, the RBF-FD method and RBF-PUM, employ a sequence of interpolation problems to discretize derivatives, where the interpolation problems are restricted to many small regions covering the computational domain. The difference between the methods can, roughly speaking, be understood from the fact that the RBF-FD method uses one local interpolation problem per node, where the solution at the node is evaluated directly from its corresponding local interpolation problem. At the same time, RBF-PUM uses one local interpolation problem per several nodes, where each local interpolation problem is in addition multiplied by a compactly supported partition of unity weight function, and a sum over all local problems is needed to evaluate the solution at one node. In [59] Shankar evolved the RBF-FD method to an overlapped RBF-FD method, by reducing the number of local interpolants from one local interpolant unique to one node, to one local interpolant unique to several nodes, which is in a sense, similar to RBF-PUM, but there is no utilization of an additional multiplication by a compactly supported partition of unity weight functions and a sum over all local interpolants, as in RBF-PUM. The RBF-FD method and RBF-PUM have mainly been used in a collocation setting to convert a PDE into an algebraic system of equations [18, 29]. In [45] the authors were the first to formulate an oversampled (least-squares) RBF-

PUM and experimentally studied its stability and convergence properties for an elliptic model problem.

A significant milestone is when the properties of the RBF-FD method were enhanced by basing the local interpolation problems on the PHS basis augmented with a high-order polynomial basis. The combination of the PHS basis and the polynomial basis is surveyed in Section 1.3.

In this thesis, we formulate an oversampled (least-squares) RBF-FD method for solving elliptic and hyperbolic PDEs and study the method's stability and convergence properties from a theoretical and an experimental point of view.

1.3 Stabilization challenges in the radial basis function methods

Radial basis function methods can be prone to different instabilities, some of which have already been resolved by different researchers. In this section, we provide an overview of a few different kinds of instabilities and give references to the existing stabilization techniques.

Stabilization of the radial basis function interpolants in the flat limit $\varepsilon \to 0$

Even if we do not use ε-dependent RBFs in the present thesis, it is relevant to mention a fascinating phenomenon related to the shape parameter, which is that when ε-dependent RBFs are on their way to becoming flat (flat limit: $\varepsilon \to 0$), the RBF interpolant becomes increasingly ill-conditioned. However, the error of the interpolation is often smaller in this regime compared with the regime when ε is large, and the RBF interpolant is well-conditioned [57]. There are two main approaches for choosing ε. The first is to fix ε to a number where ill-conditioning is not preventing the interpolation problem from being uniquely solvable on a computer, and then gradually increase the number of nodes N to converge the interpolant towards the true function that is interpolated. As N increases, the fixed ε is effectively becoming smaller relative to the internodal distance, and then the conditioning of the interpolation problem increases. Consequently, the interpolant converges for a while, but then when the conditioning becomes too large, the round-off errors make the convergence curve diverge. The second approach is to scale ε with N such that $\varepsilon N^{-1/d} = \text{constant}$ as $N \to \infty$. At some point, as $N \to \infty$, the shape parameter then becomes large, and the radial basis function may lose the ability to improve the interpolation of a function. In this case, there is a saturating effect in the convergence of the approximation error from a point where N is large enough.

In the 1990s, researchers thought of the above behavior as an uncertainty principle that is impossible to circumvent. However, in 2002, it was shown in [15] due to Driscoll and Fornberg that a one-dimensional multiquadric RBF interpolant takes a polynomial basis form in the limit $\varepsilon \to 0$. Since it is known that the polynomial basis is generally well behaved, it no longer made sense to assume that RBF interpolants were convicted to severe ill-conditioning in the flat limit. This observation, along with its generalization to other types of RBFs [26, 43], created momentum for developing stable algorithms for computing RBF interpolants in the flat limit. The first stable algorithm created was presented in [25] (RBF-CP) in 2004 due to Fornberg and Wright, with many stable algorithms to follow in later years: RBF-QR [24, 22, 44] respectively in 2007, 2011 and 2013, RBF-RA [76] in 2017, RBF-QR method based on HermiteGF expansion [41] in 2019, to name a few.

Augmentation of radial basis function interpolants using polynomials

Throughout the years, researchers started to augment RBF interpolants using multivariate monomial basis functions $\bar{p}_k$, $k = 1,..,m$, of degree D_m, where $m = \binom{D_m+d}{d}$. The objective was to enforce exactness of the interpolant for both RBFs and the monomial basis functions. An RBF interpolant augmented by monomial basis functions is given by:

$$\begin{aligned} s(y) &= \sum_{k=1}^{N} c_k \Phi_k(y) + \sum_{k=1}^{m} \lambda_k \bar{p}_k(y) \\ &\text{subject to} \sum_{k=1}^{N} c_k \bar{p}_r(x_k) = 0 \quad r = 1,..,m. \end{aligned} \tag{1.2}$$

Here λ_k, $k = 1..,m$, are Lagrange multipliers. The result of using (1.2) to construct an interpolation problem at nodes x_i, $i = 1,..,N$, is an indefinite system of equations. For all RBFs that are conditionally positive definite of order smaller than $D_m - 1$, the system has a unique solution, as long as the nodes are distinct and not located on lower dimensional manifolds [11, 17].

Initially, in the 1990s, certain RBF interpolants were augmented with a low-order monomial basis for theoretical reasons [17]. For example, an interpolation problem constructed using multiquadrics was always well-posed in practice, but it was hard to show that theoretically. The reason is that the interpolation matrix had one eigenvalue that was positive, while all others were negative. To theoretically explore the invertibility of the matrix A, it was beneficial to work with a definite A because such a matrix can form an inner product $c^T Ac \leq 0$ for any vector c. In other words, all eigenvalues need an equal sign (negative in our case), and the question then is whether the inner product is always negative/positive (A invertible), or whether the inner product

allows for 0 values when a vector $c \neq 0$ (A not invertible). Researchers have found that the multiquadric interpolation matrix is made strictly definite under an augmentation using a constant monomial term (monomial basis of degree $D_m = 0$), and then the well-posedness of the interpolation problem was easier to establish [50, 52]. Analogously, an interpolation matrix formed by using a polyharmonic spline of degree $k = 1, 3, 5, ..$ is made strictly definite under an augmentation with polynomials of degree $D_m = k - 1$ [17].

Polyharmonic splines are a particularly interesting case of RBFs, as they are ε-invariant. As opposed to many other RBF types, polyharmonic splines have a finite smoothness, i.e., a PHS of an odd degree k belongs to C^{k-1}. The condition numbers of the interpolation matrices constructed using PHS are typically well behaved for a fixed k, and only increase algebraically as $N \to \infty$, as opposed to for example interpolation matrices constructed using Gaussian RBFs or multiquadric RBFs of which the condition number increases exponentially as $N \to \infty$ [4] . The convergence trend as $N \to \infty$ when interpolating a smooth function using PHS is of order $\frac{k}{2} + 1$ [34].

During the second half of the 2010s, it became a standard to augment a low-order PHS (normally $k = 3$) with monomials of high degree (large D_m) [3, 19, 8, 7, 5]. The main reason for that was to employ the high-order polynomial exactness that essentially controls the order of the convergence. At the same time, the PHS basis helps to reduce the approximation error by a constant, compared to the local polynomial interpolation [19]. Additional benefits are reduced oscillations of the interpolation close to the boundary [8], and improved stability properties of RBF collocation discretizations of some PDEs when PHS and polynomials are used to generate finite difference stencil weights with scattered nodes [7].

Throughout the present thesis, PHS of degree $k = 3$, augmented with a high degree monomial basis, is the local interpolation setting that we use to construct the global function spaces where we look for numerical solutions to PDEs.

Stabilization of radial basis function methods applied to time-dependent hyperbolic partial differential equations

Hyperbolic time-dependent partial differential equations are used to describe transport phenomena, i.e., their solutions propagate an initial condition function without change in the energy of the initial condition function. This thesis considers first-order hyperbolic time-dependent problems, which contain first derivative in time and first derivatives in space. There are two types of instabilities for many of the numerical discretization methods that can occur as the numerical solution is advanced in time.

The first type of instability is implicitly related to the spurious eigenvalue spectra of a linear discrete divergence operator. The spectrum of the linear

discrete divergence operator supplied by inflow boundary conditions must not contain positive eigenvalues, as that would cause an unbounded growth of the numerical solution as time goes to infinity. While some of the numerical methods are, in this sense, stable by construction, for example, Galerkin finite element methods or summation-by-parts finite difference methods, the RBF-FD method and RBF-PUM were experimentally found unstable and require the addition of stabilization terms. One of the standard stabilization terms for the collocation RBF methods is to apply an upwinding viscosity operator [69], which only allows the numerical solution to have a first-order accuracy, no matter how smooth the initial condition is. Hyperviscosity (high-order viscosity operator) is another common stabilization term [23], which allows the numerical solution to have a higher-order accuracy if the initial condition is smooth enough.

The second type of instability is specific to nonlinear hyperbolic PDE problems. As time goes to infinity, the exact solutions to these problems develop a shock (discontinuity). Each continuous finite-dimensional approximation of a shock induces an overshoot over the shock, also referred to as the Gibbs phenomenon.

In this thesis, we explain why some RBF methods are subject to instabilities of the first type. Furthermore, we use a residual-based viscosity method borrowed from the finite element community [53, 65] to locally ameliorate the instabilities of the second type.

1.4 Applications addressed using radial basis function methods

Radial basis function methods have been used to solve PDE problems arising from various types of applications. Examples include: ice sheet models [13, 1], financial engineering models [56, 60, 51], metal casting models [70, 33], geophysical models [75, 20, 21, 6, 49], phononic crystal models [78], contact models [63], combustion models [9], benchmark elasticity models [67, 62] and many others.

In this thesis, we apply the RBF-FD method to a benchmark linear elasticity model where the computational domain is the thoracic diaphragm which is the primary muscle of the respiratory system in a human being. Another application that we consider is a benchmark model of compressed gas dynamics, governed by the Euler system of equations.

1.5 Novel contributions of the present thesis

The main thread of the present thesis is the RBF-FD method for solving PDEs. We present advances within the method development and the theoretical anal-

ysis of the method, and solve applications in biomechanics and fluid mechanics. We also discuss RBF-PUM and Kansa's global RBF method in one of the papers.

In Paper I we make developments of the RBF-FD method in terms of stability properties when solving an elliptic model problem with derivative-type boundary conditions in combination with Dirichlet boundary conditions. We highlight that the basis functions spanning the RBF-FD function space over a computational domain are only piecewise continuous. Another contribution is an associated theoretical study.

In Paper II we develop an unfitted RBF-FD method and solve an elliptic PDE on highly complex domains such as the thoracic diaphragm. The key benefit is that the computational nodes do not need to conform to the boundary of the domain, but instead, extend outside of the domain, enabling a simpler node generation handling. We observed a smaller approximation error around the boundaries of the domain when the order of the method is large, compared with the approximation error when using a classical, fitted RBF-FD method. We also provide a computational study evaluating different criteria to ensure the linear independence of the basis functions over the interior of the domain, a common problem of the unfitted type of methods.

In Paper III we use the unfitted RBF-FD method to compute solutions over a simplified thoracic diaphragm geometry, Furthermore, we employ data smoothing and boundary condition smoothing for obtaining high-order convergence when solving an elastic system of PDEs. We provide a numerical convergence study, where the finite element method is used to provide a reference solution.

In Paper IV we explore the stability properties behind the RBF-FD method, Kansa's method, and RBF-PUM when they are used to solve a linear time-dependent hyperbolic PDE. We theoretically show that Kansa's method and RBF-PUM can be stable under a sufficient oversampling of the system of equations. We also show that the RBF-FD numerical solution's insufficient regularity prevents the RBF-FD method from being stable in time, no matter the amount of oversampling. Numerical experiments confirm the theoretical observations.

In Paper V we use the residual viscosity method to locally stabilize the Gibbs phenomenon present in the RBF-FD solutions to shock-inducing nonlinear time-dependent conservation laws. We solve benchmark problems involving the linear advection equation, Burger's equation, and the compressible Euler system of equations.

2. Partial differential equation models

In this thesis we focus on two types of PDE problems. The first is a linear stationary PDE problem formulated over a domain $\Omega \subset \mathbb{R}^d$, $d = 2,3$:

$$\begin{aligned} \mathscr{L}u(y) &= f(y), \quad y \in \Omega \\ \mathscr{B}u(y) &= g(y), \quad y \in \partial\Omega, \end{aligned} \tag{2.1}$$

where $\mathscr{L}$ is a linear differential operator with a corresponding data function $f(y)$, and $\mathscr{B}$ is a linear boundary operator with a corresponding boundary data function $g(y)$. We consider the problem in the scalar and the system setting, where the first setting corresponds to a Poisson equation and the second to a linear elasticity problem. We use either purely Dirichlet boundary conditions or mixed boundary conditions, i.e., a Dirichlet boundary condition and a Neumann-type boundary condition imposed on two disjoint parts of $\partial\Omega$, that is, $\partial\Omega_0$ and $\partial\Omega_1$ respectively.

We also solve a time-dependent hyperbolic PDE problem:

$$\begin{aligned} \partial_t u(y,t) &= -\nabla \cdot F(u(y,t),t), && y \in \Omega \\ u(y,t) &= g(y,t), && y \in \Gamma_{\text{inflow}}, \\ u(y,0) &= u_0(y), && y \in \bar{\Omega}, \end{aligned} \tag{2.2}$$

where $t > 0$ is time, F is a (non)linear flux that does not include any physical viscous forces, and the second and the third constraint are an inflow boundary condition and an initial condition respectively. We again consider the problem in the scalar setting and the system setting, where the first corresponds to a linear advection equation, and the second to the Euler system of equations.

3. Constructing an RBF function space

RBF methods are often explained through a sequence of steps that directly lead to the construction of differentiation matrices which then replace the exact derivatives in a PDE. Each row of a differentiation matrix is referred to as a set of (differentiation) weights. In the present thesis, we take a slightly more general approach and describe the RBF methods by providing a sequence of steps that lead to a set of cardinal basis functions which span an RBF function space. The line of thinking is then to seek a solution to a PDE within the constructed RBF function space enabling a broader perspective when addressing the stability properties of the RBF methods.

A numerical solution u_h to a PDE over an open and bounded domain $\Omega \subset \mathbb{R}^d$, $d = 1,2,3,\ldots$, is computed using an ansatz:

$$u_h(y) = \sum_{k=1}^{N} u(x_k)\Psi_k(y), \quad u_h(y,t) = \sum_{k=1}^{N} u(x_k,t)\Psi_k(y), \tag{3.1}$$

where the first ansatz is used for stationary PDE problems and the second ansatz is used for time-dependent PDE problems. Here $\Psi_k(y)$, $k = 1,..,N$, are the cardinal basis functions constructed in different ways depending on the choice of the RBF method, and $u(x_k)$ or $u(x_k,t)$, $k = 1,..,N$, are the unknown nodal values at the nodes $x_k \in \Omega$, and $y \in \Omega$ is an evaluation point. We use

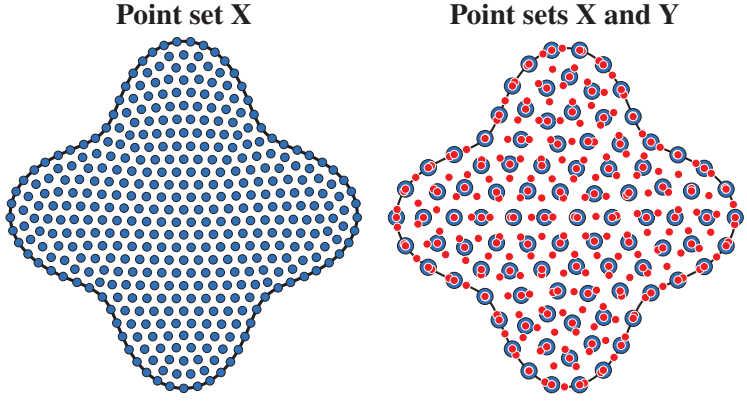

Figure 3.1. Left: an example point set X (blue markers). Right: an example point set X (blue markers) together with the evaluation point set Y (red markers), where the oversampling parameter is set to $q = 4$.

two types of point sets: the nodal point set $X = \{x_i\}_{k=1}^{N}$ and the evaluation

point set $Y = \{y_j\}_{j=1}^{M} = Y_\Omega \cup Y_{\partial\Omega}$ with $M = qN$, $q \geq 1$, where q is referred to as the oversampling parameter, and where Y_Ω and $Y_{\partial\Omega}$ correspond to sets of evaluation points placed in the interior of the domain, and on the boundary of the domain respectively. The nodal point set is used to construct the cardinal basis functions. The evaluation point set is used to sample the PDE with the intention to convert the PDE into either a square or a rectangular system of algebraic equations, which we solve for the unknown nodal values. The internodal distances in the two point sets are defined as the radius of the largest ball that fits inbetween the points:

$$h = \sup_{x\in\Omega} \min_{x_j\in X} \|x - x_j\|_2, \quad h_y = \sup_{y\in\Omega} \min_{y_j\in Y} \|y - y_j\|_2. \tag{3.2}$$

In this chapter, we focus on constructing the cardinal basis functions Ψ_k, $k = 1,..,N$, that span the function space within which we are seeking a numerical solution of the form (3.1). We use three commonly used RBF methods to construct the cardinal basis functions: Kansa's RBF method, the RBF partition of unity method (RBF-PUM), and the RBF generated finite difference (RBF-FD) method. The methods are different to each other in terms of (i) the support of the cardinal basis functions and (ii) the continuity of the cardinal basis functions. In this thesis, we focus on the RBF-FD method, but we also consider Kansa's RBF method and RBF-PUM in one of the papers. The methods are described in the sections that follow. To make the discussion general enough, we allow time dependence of the unknown coefficients. However, when using the methods for stationary PDE problems, the time dependence can simply be dropped, and the derivation remains identical. We first show how to form the

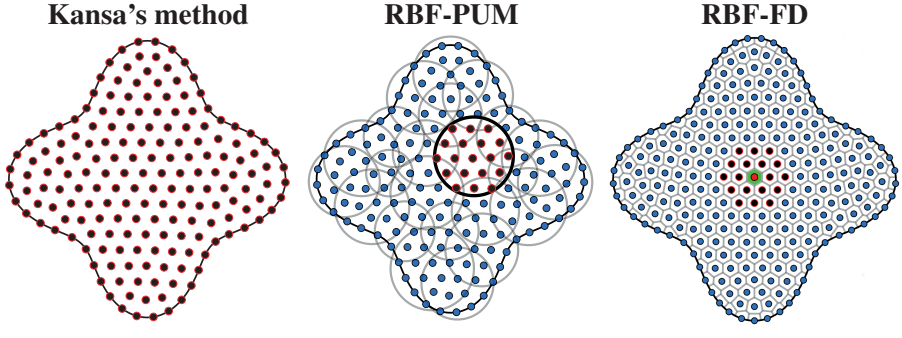

Figure 3.2. Nodes (blue points) and different node supports (black points with red edges) specific to three RBF methods: Kansa's RBF method (global support), the RBF partition of unity method (patch support) and the RBF generated finite difference (RBF-FD) method (stencil support). The green area in the RBF-FD method case illustrates the region to which the stencil approximation is further restricted when evaluating the numerical solution.

cardinal basis functions using Kansa's method, and then extend that to RBF-PUM and the RBF-FD method. We also provide a discussion about the global

regularity properties of the cardinal basis functions constructed using each of the methods.

3.1 Kansa's global RBF method

In Kansa's method case we form an interpolant over Ω using radial basis functions $\phi_l(x)$, $l = 1,..,N$ and (potentially) the monomial basis, $\bar{p}_k(x)$, $k = 1,..,m$:

$$\begin{aligned} u_h(y,t) &= \sum_{l=1}^{N} c_l(t)\phi_l(y) + \sum_{k=1}^{m} \lambda_k(t)\bar{p}_k(y), \\ &\text{subject to } \sum_{l=1}^{N} c_l(t)\bar{p}_k(x_l) = 0, \quad k = 1,..,m, \end{aligned} \tag{3.3}$$

where $c_l(t)$ are the unknown interpolation coefficients, $\lambda_k(t)$ the unknown Lagrange multipliers, and where the number of monomial terms is $m = \binom{D_m+2}{2}$, where D_m is the degree of the monomial basis. We use the cubic polyharmonic spline (PHS) radial basis functions $\phi_l(x) = \|x - x_l\|_2^3$. Requiring the interpolation conditions $u_h(x_i,t) = u(x_i,t)$, $i = 1,..,N$, to hold, where $x_i \in X$ and $u(x_i,t)$ are the unknown nodal values, gives a system of equations on matrix-vector form:

$$\underbrace{\begin{pmatrix} A & P \\ P^T & 0 \end{pmatrix}}_{:=\tilde{A}} \begin{pmatrix} \underline{c}(t) \\ \underline{\lambda}(t) \end{pmatrix} = \begin{pmatrix} \underline{u}(X,t) \\ 0 \end{pmatrix} \quad \Leftrightarrow \quad \begin{pmatrix} \underline{c}(t) \\ \underline{\lambda}(t) \end{pmatrix} = \tilde{A}^{-1} \begin{pmatrix} \underline{u}(X,t) \\ 0 \end{pmatrix}. \tag{3.4}$$

Here $A_{jl} = \phi_l(x_j)$ for indices $j,l = 1,..,N$ and $P_{jk} = \bar{p}_k(x_j)$ for indices $k = 1,..,m$ and $u_j = u(x_j,t)$. Reusing the computed coefficients inside (3.3), only keeping the first N terms, and disregarding the $N+1,..,N+m$ terms, gives:

$$\begin{aligned} u_h(y,t) &= \underbrace{\left(\phi_1(y),..,\phi_N(y),\, \bar{p}_1(y),..,\bar{p}_m(y)\right)}_{:=b(y)} \begin{pmatrix} \underline{c}(t) \\ \underline{\lambda}(t) \end{pmatrix} = \left(b(y)\tilde{A}^{-1}\right)_{1:N} \underline{u}(X,t) \\ &= \sum_{k=1}^{N} u(x_k,t) \left[b(y,X)\tilde{A}^{-1}(X,X)\right]_k \equiv \sum_{k=1}^{N} u(x_k,t)\Psi_k(y). \end{aligned} \tag{3.5}$$

The cardinal basis functions Ψ_i, $i = 1,..,N$, constructed by using Kansa's method are then given through (3.5).

3.2 The RBF partition of unity method (RBF-PUM)

When using RBF-PUM the computational domain is subdivided into overlapping patches $\cup_{j=1}^{N_p} \Omega^{(j)} \supset \Omega$, where an interpolation problem as in (3.4) is then

solved on each patch, instead of on the whole Ω. The local solution over each patch, $u_h^{(j)}$, is spanned by a set of local cardinal basis functions $\psi_k^{(j)}$ formed analogously to (3.5), where:

$$u_h^{(j)}(y,t) = \sum_{k=1}^{n^{(j)}} u(x_k^{(j)},t) \left[b(y,X^{(j)}) \tilde{A}^{-1}(X^{(j)},X^{(j)}) \right]_k \equiv \sum_{k=1}^{n^{(j)}} u(x_k^{(j)},t) \psi_k^{(j)}(y). \tag{3.6}$$

Here $n^{(j)}$ is the number of nodes $X^{(j)} \subset X$ contained in the patch with index j. To further define the solution over all of Ω, we then blend the local solutions over the patches together by using compactly supported partition of unity weight functions:

$$u_h(y,t) = \sum_{j=1}^{N_p} w_j(y) u_h^{(j)}(y,t), \tag{3.7}$$

where each $w_j(y)$ is constructed using Shepard's method [61] employing Wendland's compactly supported functions [72]. We now introduce: (a) the set $J(i)$ of all patches that contain x_i, (b) an index operator $\kappa(j,i)$, which gives the local index of x_i inside the patch $\Omega^{(j)}$. The global RBF-PUM solution is then:

$$\begin{aligned} u_h(y,t) &= \sum_{j=1}^{N_p} w_j(y) \sum_{k=1}^{n^{(j)}} u(x_k^{(j)},t) \psi_k^{(j)}(y) \\ &= \sum_{i=1}^{N} u(x_i,t) \sum_{j \in J(i)} w_j(y) \psi_{\kappa(j,i)}^{(j)}(y) \equiv \sum_{i=1}^{N} u(x_i,t) \Psi_i(y). \end{aligned} \tag{3.8}$$

3.3 The RBF-generated finite difference (RBF-FD) method

In the RBF-FD case each node $x_i \in X$ is associated with a neighborhood of the n closest nodes $X^{(i)} \subset X$ (a stencil), see Figure 3.2. The interpolation problem (3.4) is then solved on each stencil. The local solution over a stencil is formulated analogously as in the RBF-PUM case over a patch (3.6). In this case, $\psi_k^{(i)}$ are the RBF-FD local cardinal basis functions that span the local function space over each stencil. To get a globally defined function space, each $u_h^{(i)}$ is restricted to a small non-overlapping region (a Voronoi cell) centered around the corresponding $x_i \in X$, see Figure 3.2:

$$u_h(y,t) = u_h^{(\rho(y))}(y,t), \quad i = 1,..,N, \tag{3.9}$$

where $\rho(y)$ is an index mapping defined by:

$$\rho(y) = \arg\min_{i \in [1,N]} \|y - x_i\|_2. \tag{3.10}$$

An equivalent form to (3.9), which uses the global RBF-FD cardinal basis functions, is:

$$u_h(y,t) = \sum_{i=1}^{N} u(x_i,t)\, \psi^{(\rho(y))}_{\kappa(\rho(y),i)}(y) \equiv \sum_{i=1}^{N} u(x_i,t)\Psi_i(y),$$

where $\kappa(\rho(y),i)$ is an index operator that gives the local index of x_i inside the stencil point set $X^{(\rho(y))}$. A MATLAB code for generating differentiation matrices (derivatives of the evaluated RBF-FD cardinal basis functions) and evaluation matrices (the evaluated RBF-FD cardinal basis functions) is provided in [68]. An algorithm for generating the matrices is provided in Paper III, Section 4.

3.4 Regularity of the cardinal basis functions, and the associated function spaces

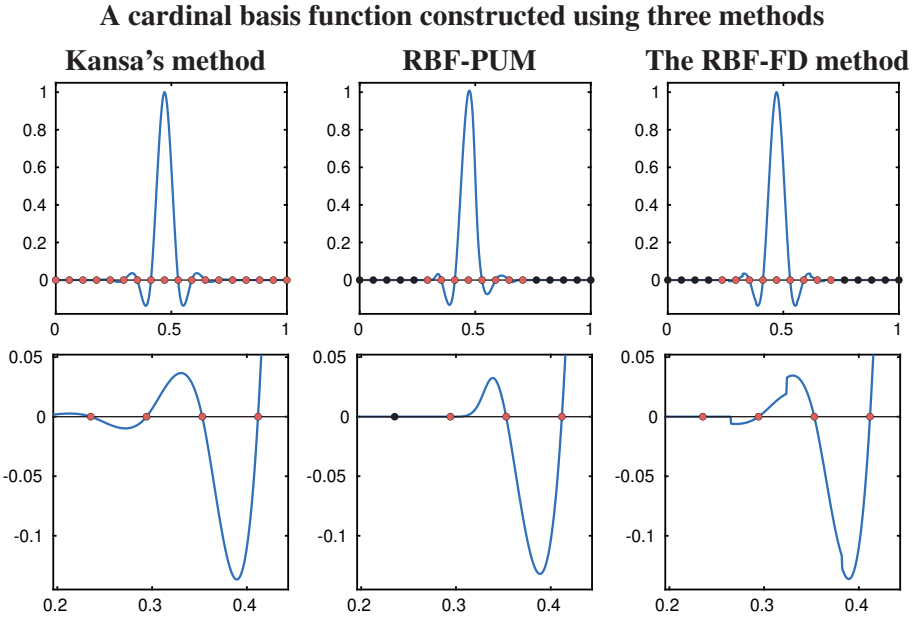

Figure 3.3. Three examples of cardinal functions centered at a node in the middle of the domain, where each cardinal function is constructed either using Kansa's method, RBF-PUM or the RBF-FD method. The first row of plots shows a full cardinal basis function. The second row shows the corresponding close-ups. Nodes colored in red mark the region where a cardinal basis function has non-zero support.

When deriving stability and convergence estimates for a numerical solution using a discretization, it is important to understand what regularity properties

the constructed cardinal basis functions have. This way, we can recognize which space of functions the cardinal basis functions belong to, and then prepare the theoretical analysis accordingly. Since our numerical solution is computed as (3.1), our finite dimensional function space V_h is $V_h = \text{span}(\{\Psi_i\}_{i=1}^N)$. The regularity properties of V_h are then given by the regularity of Ψ_i, $i = 1,..,N$. However, these functions are constructed differently depending on the RBF method of choice, as described in the sections above. As discussed in Paper IV and in Paper I we have the following spaces per each RBF method. Kansa's method and RBF-PUM construct $V_h \subset W_2^{k+1}(\Omega)$, $k \geq 0$, where the smoothness order k for Kansa's method is governed by the regularity of the radial basis functions, whereas in the RBF-PUM case, k is governed by the minimal regularity of the partition of unity weight functions and the radial basis functions. In the RBF-FD case we only have a piecewise continuous space:

$$V_h = \{u_h \in L_2(\Omega) \,|\, u_h \in W_2^{k+1}(K_i), \quad \cup_{i=1}^N K_i = \Omega\}, \quad k \geq 0. \tag{3.11}$$

Here K_i is a Voronoi cell centered around the corresponding $x_i \in X$. The local regularity degree k, over a Voronoi region, is governed by the regularity of the radial basis functions. It is very important to emphasize that even if the RBF-FD cardinal basis functions are discontinuous, all cardinal basis functions still share degrees of freedom with each other, which for example, is not the case for the discontinuous Galerkin (DG) function spaces that are also in a subset of $L_2(\Omega)$. Examples of cardinal basis functions constructed using all three RBF methods are plotted in Figure 3.3, from where it is possible to observe that the RBF-FD cardinal basis functions contain jumps, while Kansa's and the RBF-PUM cardinal basis functions are smooth.

4. Collocated and oversampled discretizations of PDEs

A collocation type of PDE discretization is the standard type to use when searching for numerical solutions using RBFs. In the present thesis, we instead use an oversampled type of PDE discretization. In this chapter, we discretize two scalar PDE problems using both types. In addition, we outline the properties of the oversampled setting that make it possible to perform a theoretical analysis of the RBF discretizations utilizing the estimation techniques normally used in the finite element community.

4.1 Discretization of a stationary PDE problem

Consider the PDE problem from (2.1). Using the first ansatz from (3.1) in (2.1), and then sampling the PDE at the evaluation point set of size $M = M_\Omega + M_{\partial\Omega}$, we have:

$$\begin{aligned} \beta(y_k) \sum_{i=1}^{N} u_h(x_i) \mathscr{L}\Psi_i(y_k) &= \beta(y_k) f(y_k), \quad y_k \in Y_\Omega, \\ \beta(y_k) \sum_{i=1}^{N} u_h(x_i) \Psi_i(y_k) &= \beta(y_k) g(y_k), \quad y_k \in Y_{\partial\Omega}, \end{aligned} \tag{4.1}$$

where we also multiplied all equations by a scaling factor $\beta(y)$, defined by:

$$\beta(y) = \begin{cases} h^{-\frac{1}{2}} h_y^{\frac{d-1}{2}}, & y \in \partial\Omega, \\ h_y^{\frac{d}{2}}, & y \in \Omega, \end{cases} \tag{4.2}$$

where h and h_y are defined in (3.2). These scaling factors were derived by relating the discrete least-squares projection of (4.1) which employs ℓ_2 inner products, to a continuous least-squares projection which employs L_2 inner products.

The matrix-vector form of (4.1) is $\bar{D}_h u_h = \bar{F}$. When $Y = X$, then $\bar{D}_h$ is square by construction, and the solution is given by $u_h = \bar{D}_h^{-1} \bar{F}$. Here the resulting residual minimizing framework is called collocation, i.e., after the solution is computed, the pointwise residual at point set $X = Y$ of the discretized PDE is 0. In this case the scaling $\beta(y)$ does not play any role in the

properties of the system of equations. When $Y \neq X$ and $M > N$ then the resulting system of equations is rectangular, the solution is in this case given by $u_h = \bar{D}_h^+ \bar{F}$, where $\bar{D}_h^+ = (\bar{D}_h^T \bar{D}_h)^{-1} \bar{D}_h^T$ is the pseudo-inverse of $\bar{D}_h$ defined by employing a discrete least-squares projection. The resulting residual at the point set Y is in this case non-zero, and $\beta(y)$ now plays a significant role in terms of the stability properties of the numerical solution and also the overall approximation properties of the numerical solution.

4.2 Discretization of a time-dependent PDE problem

Now we consider the PDE problem from (2.2). Using the second ansatz from (3.1) inside (2.2), and then sampling the PDE at the evaluation point set of size M, we first discretize the PDE in space to arrive at a system of ODEs:

$$\beta(y_k) \sum_{i=1}^{N} \partial_t u_h(x_i,t)\, \Psi_i(y_k) = -\beta(y_k) \sum_{i=1}^{N} \left(F_1^{(i)} \nabla_1 + F_2^{(i)} \nabla_2 \right) \Psi_i(y_k), \qquad k = 1,..,M, \tag{4.3}$$

where ∇_r, $r = 1,2$ is the derivative with respect to the r-th component of y, and $F_r^{(i)} = F_r(u_h(x_i,t),t)$, $r = 1,2$, are the two components of the flux term F evaluated at $x_i \in X$ and $t > 0$. The matrix-vector form of (4.3) is $\bar{E}_h \partial_t u_h = \bar{D}_h u_h$. When $Y = X$ (collocation case) then $\Psi_i(y_k) = 1$ when $k = i$, and thus $\bar{E}_h$ is a scaled identity matrix. In this case we directly use classical explicit Runge-Kutta 4 methods to advance the solution of the ODE system in time. When $Y \neq X$ and $M > N$, then the involved matrices are rectangular. We then project (4.3) onto the column space of $\bar{E}_h$ by multiplication with $\bar{E}_h^T$ which gives $\bar{E}_h^T \bar{E}_h \partial_t u_h = \bar{E}_h^T \bar{D}_h u_h$. To recover an explicit dependence on the time derivative of u_h, we invert the mass matrix and obtain $\partial_t u_h = (\bar{E}_h^T \bar{E}_h)^{-1} (\bar{E}_h^T \bar{D}_h) u_h$. In practice, however, we do not invert the mass matrix directly but instead compute the solution to the system of ODEs by the conjugate gradient iterative method in each timestep of the classical Runge-Kutta 4 method.

The boundary condition from (2.2) is enforced exactly by removing the unknown nodal coefficient values corresponding to the location of the inflow boundary condition.

4.3 Properties of the oversampled PDE discretizations from a variational point of view

Consider a stationary PDE (2.1). The discretized PDE is the system of equations $\bar{D}_h u_h = \bar{F}$ given through (4.1) and a further discussion in Section 4.1. Let $M > N$, so that $\bar{D}_h$ is rectangular. We are now going to demonstrate that

the rectangular system of equations arising from the oversampled PDE discretization (4.1) is very closely related to a variational problem, in which the integrals are replaced by weighted sums, and where the weighted sums represent an inexact quadrature rule. To make an illustration, we project our rectangular system of equations onto the column space of D_h, resulting in the normal equations:

$$\bar{D}_h^T \bar{D}_h u_h = \bar{D}_h^T \bar{F}, \tag{4.4}$$

where the new system size is $N \times N$. We note that looking at the components of the matrices involved in (4.4) by using (4.1) and (4.2) where we set $d = 2$, we have:

$$\begin{aligned}(\bar{D}_h^T \bar{D}_h)_{ij} &= h_y^2 \sum_{y \in Y_\Omega} \mathscr{L}\Psi_i(y)\, \mathscr{L}\Psi_j(y) + h^{-1} h_y \sum_{y \in Y_{\partial\Omega}} \Psi_i(y)\, \Psi_j(y) \\ &\equiv (\mathscr{L}\Psi_i, \mathscr{L}\Psi_j)_{\ell_2(\Omega)} + h^{-1} (\Psi_i, \Psi_j)_{\ell_2(\partial\Omega)},\end{aligned} \tag{4.5}$$

and also:

$$\begin{aligned}(\bar{D}_h^T \bar{F})_j &= h_y^2 \sum_{y \in Y_\Omega} f(y)\, \mathscr{L}\Psi_j(y) + h^{-1} h_y \sum_{y \in Y_{\partial\Omega}} g(y)\, \Psi_j(y). \\ &\equiv (f, \mathscr{L}\Psi_j)_{\ell_2(\Omega)} + h^{-1} (g, \Psi_j)_{\ell_2(\partial\Omega)},\end{aligned} \tag{4.6}$$

thus, discrete inner products are governing our system of equations. Each equation of the system in (4.4) is then:

$$\begin{aligned}\sum_{i=1}^{N} u(x_i)\, (\mathscr{L}\Psi_i, \mathscr{L}\Psi_j)_{\ell_2(\Omega)} + h^{-1} \sum_{i=1}^{N} u(x_i)\, (\Psi_i, \Psi_j)_{\ell_2(\partial\Omega)} = \\ = (f, \mathscr{L}\Psi_j)_{\ell_2(\Omega)} + h^{-1} (g, \Psi_j)_{\ell_2(\partial\Omega)} \\ j = 1, .., N,\end{aligned} \tag{4.7}$$

where we further denote that the associated bilinear form and the associated linear functional are defined by:

$$\begin{aligned}a_h(u_h, v_h) &= (\mathscr{L}u_h, \mathscr{L}v_h)_{\ell_2(\Omega)} + h^{-1} (u_h, v_h)_{\ell_2(\partial\Omega)}, \\ l(v_h) &= (f, \mathscr{L}v_h)_{\ell_2(\Omega)} + h^{-1} (g, v_h)_{\ell_2(\partial\Omega)}.\end{aligned} \tag{4.8}$$

The PDE problem equivalent to (4.4) then reads. Find u_h with $v_h = \Psi_j$, $j = 1, .., N$, such that:

$$a_h(u_h, v_h) = l(v_h).$$

Here we note that the second term of $a_h(u_h, v_h)$ and $l(v_h)$ is a penalty that weakly imposes the Dirichlet boundary condition. We have that $u_h, v_h \in V_h$, where a discussion about the properties of V_h depending on which RBF methods construct Ψ_i, $i = 1, .., N$, is provided in Section 3.4

Showing well-posedness of a discrete problem through the Riesz representation theorem for a symmetric a_h [10] or through the Lax-Milgram lemma for

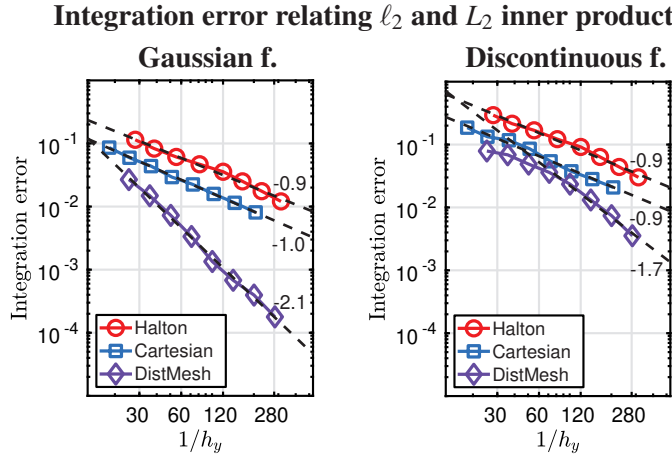

Figure 4.1. Integration error relating a discrete ℓ_2 inner product to an L_2 inner product, measured as a function of the inverse mean internodal distance in the point set Y, for two different integrands: a Gaussian function (left plot) and a discontinuous function concatenated from local trigonometric functions (right plot). Three different point sets Y are used to compute the integration error.

a non-symmetric a_h [10] is more convenient when the bilinear form is employing inner products over an L_2 space instead of a finite-dimensional ℓ_2 space, as in our case (4.7). The convenience is attributed to a vast amount of inequalities available for making estimates using the L_2 inner products, such as Poincare's inequality, trace inequalities, inverse inequalities, and other inequalities [10]. However, in (4.8), we can relate the ℓ_2 inner products to L_2 inner products and then perform the analysis on those L_2 inner products, as is clasically done in those finite element methods that are employing variational principles. A piecewise L_2 inner product is defined by:

$$(u_h, v_h)_{L_2^*(\Omega)} = \sum_{K_i \in \Omega} \int_{K_i} u_h v_h \, dK_i,$$

where $K_i \in \Omega$ is a Voronoi cell centered around a node x_i, $i = 1, .., N$, such that $\cup_{i=1}^{N} K_i = \Omega$. In Paper IV we derived a relation between the two inner products in two spatial dimensions for a point set Y with a Cartesian distribution over a complex geometry and for $u_h, v_h \in L_2(\Omega)$ as:

$$\begin{aligned} (u_h, v_h)_{\ell_2(\Omega)} &\leq C_{\int} h^{-1} h_y \max_i \|u_h v_h\|_{L_\infty(K_i)} + (u_h, v_h)_{L_2^*(\Omega)} \\ &\equiv e_I(u_h v_h) + (u_h, v_h)_{L_2^*(\Omega)}, \end{aligned} \tag{4.9}$$

where $e_I(u_h v_h)$ is an integration error term. At least a linear convergence in h_y is also expected for quasi-uniform point sets Y, as we experimentally demonstrated in the same paper, see Figure 4.1. Coercivity of a_h, i.e. $a_h(u_h, u_h) \geq$

$\alpha^2\|u_h\|^2_{L_2^*(\Omega)}$ for $\alpha > 0$, is one of the important properties when it comes to the invertibility of the "stiffness" matrix, in our case $\bar{D}_h^T\bar{D}_h$. Combining (4.8), (4.7) and an established coercivity property, it is possible to show that:

$$a_h(u_h,u_h) = u^T\bar{D}_h^T\bar{D}_h u \geq \alpha^2\|u_h\|^2_{\ell_2(\Omega)} > 0 \Rightarrow \inf_{u^Tu=1} u^T\bar{D}_h^T\bar{D}_h u > 0.$$

The last equality involving the infimum of a discrete inner product is a definition of the smallest eigenvalue of a matrix. Coercivity then implies that the smallest eigenvalue of $\bar{D}_h^T\bar{D}_h$ is larger than 0, thus, the matrix has an inverse. However, the simplicity of proving the coercivity property heavily depends on the regularity properties of V_h (see Section 3.4).

Similar arguments as for a stationary oversampled problem can also be used for an oversampled discretization of a time-dependent problem described in Section 4.2. In two dimensions, a form equivalent to (4.7) is:

$$\sum_{i=1}^{N}\partial_t u(x_i,t)\,(\Psi_i,\Psi_j)_{\ell_2(\Omega)} = \sum_{i=1}^{N}\left([F_1(u(x_i,t))\nabla_1 + F_2(u(x_i,t))\nabla_2]\,\Psi_i,\Psi_j\right)_{\ell_2(\Omega)} \qquad j = 1,..,N. \tag{4.10}$$

By using the relation (4.9) in (4.10), this time only for the right-hand-side inner product, it is then possible to make a semi-discrete stability estimate of type:

$$\partial_t\|u_h\|^2_{\ell_2(\Omega)} \leq \underbrace{\text{boundary data}}_{\text{physics}} + \underbrace{\text{potential spurious terms}}_{\text{numerics}}.$$

The estimate is also referred to as the linear stability estimate, since it is a sufficient resource to establish the stability of numerical solutions to linear time-dependent problems with smooth data. In a nonlinear setting, the linear stability estimate is still required, but it is not sufficient to establish the overall stability of a numerical scheme. If a semi-discrete stability estimate is established, this then means that the energy of the numerical solution is only allowed to grow in time when the physical inflow boundary conditions also grow in time. Even if the semi-discrete stability setting is not covering the fully discrete case, where the time dimension is discretized in addition, it is informative enough to discover potential spurious terms coming from the spatial discretization. In Paper IV we show that for the RBF-FD method, there are two spurious terms related to the spatial discretization: (i) the jump term due to the discontinuous function space V_h, (ii) the inexact integration error term. For Kansa's RBF method and RBF-PUM, the inexact integration error term is the only spurious term.

4.4 Benefits when using an oversampled discretization over a collocated discretization, from a numerical point of view

In Paper I we constructed a function space using the RBF-FD method and used an oversampled stationary PDE discretization. We used Dirichlet and Neumann boundary conditions imposed on two disjoint parts of the computational domain, and measured the stability norm and the convergence of the approximation error under node refinement, respectively defined by:

$$\text{Stability norm } = \|\bar{E}_h\|_2 \|\bar{D}_h^+\|_2, \quad \|e\|_{\ell_2(\Omega)} = \frac{\|u_h(Y) - u_{\text{ref}}(Y)\|_{\ell_2(\Omega)}}{\|u_{\text{ref}}(Y)\|_{\ell_2(\Omega)}}. \tag{4.11}$$

An ideal stability norm stays constant independent of the internodal distance h, while the approximation error, in the Poisson problem case, decays with at least an order $p-1$, if the polynomial degree used to construct the local interpolation problems is p. Numerical results for the most basic colloca-

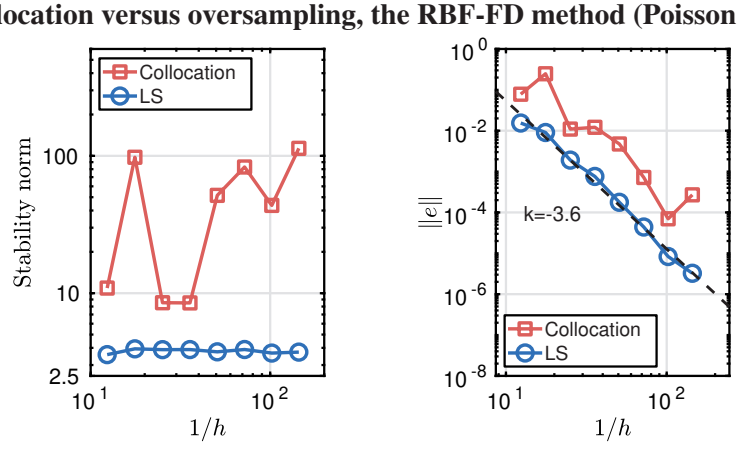

Figure 4.2. The stability norm (left) and the convergence of the approximation error under node refinement, for an oversampled RBF-FD discretization of the Poisson equation with mixed boundary conditions. The polynomial degree $p = 4$ is used to construct the stencil based approximation. The oversampling parameter is fixed to $q = 3$. The label "LS" indicates results related to the oversampled RBF-FD method, while the label "Collocation" indicates results related to the collocation RBF-FD method.

tion RBF-FD method and the most basic oversampled RBF-FD method are provided in Figure 4.2. The stability norm is nearly constant for the oversampled RBF-FD method, while it is oscillating for the collocation RBF-FD method. The convergence curve for the oversampled RBF-FD method follows a prescribed trend, which is not the case for the collocation RBF-FD method. Similar behavior was observed throughout Paper I.

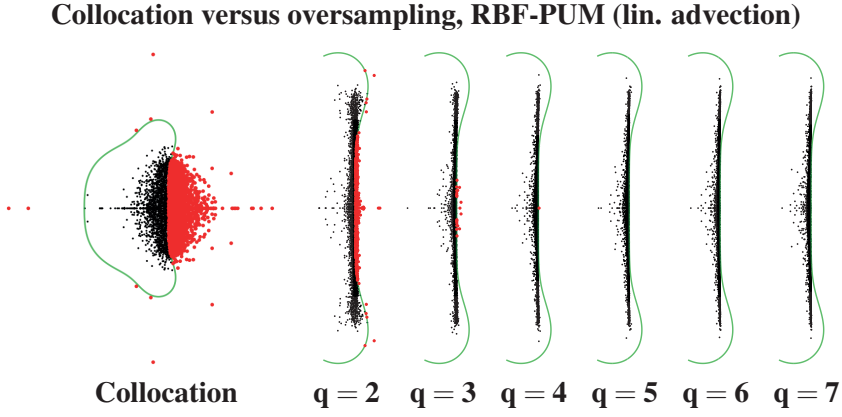

Figure 4.3. Eigenvalue spectra (black dots) of the advection operator with 0 inflow boundary conditions, when RBF-PUM is used on randomly perturbed DistMesh X points ($h = 0.03$), as the oversampling parameter q is gradually increased. The green line is the entire stability region ($q = 1$ case) or its boundary ($q > 1$ cases), of the classical explicit Runge-Kutta 4 method. The red dots are the eigenvalues that are not inside the stability region.

In Paper IV we numerically studied the effect of oversampling on the eigenvalue spectra of a linear advection operator with inflow boundary conditions. An ideal eigenvalue spectrum contains eigenvalues in the interior of the stability region of an explicit time-stepping method. In Figure 4.3 we show the eigenvalue spectrum in the RBF-PUM case, for different value of the oversampling parameter. Collocation gives many spurious eigenvalues, while the oversampling approach shifts the eigenvalues to the interior of the stability region, as q is increased. Similar behavior was also observed for Kansa's method and the jump-stabilized RBF-FD method. Oversampling did not improve the time-stability properties of the RBF-FD method if the jumps in the cardinal basis functions were not stabilized separately.

5. Unfitted radial basis function methods for solving PDEs

To illustrate the difference between a classical, fitted method for solving a PDE, and an unfitted method, we start with Figure 3.1 where the node set X is conforming to the shape of the boundary of the computational domain Ω. Constructing such a point set, with an approximately uniform internodal distance around the boundary, can already be demanding in two dimensions, and gets increasingly more demanding as the number of dimensions grow. At the same time, it is many times the case that the approximation error is smaller when the internodal distance distribution is nearly smooth. A possible alternative to construct X, visualized in Figure 5.1, is to place a node template into a box that encapsulates Ω, remove the points too far away from the boundary of Ω, and discretize the PDE at an evaluation point set Y that conforms to Ω. The internodal distance in the point set Y does not have to vary smoothly across the domain and around the boundaries. Unfitted methods are also referred to as *immersed methods*. The first method of this kind emerged in 1972 due to Peskin [55]. From then on, researchers developed many such methods, for example a Cartesian cut-cell method [77] or cut finite element (CutFEM) methods [12, 64, 31]. In Paper II, we were first to

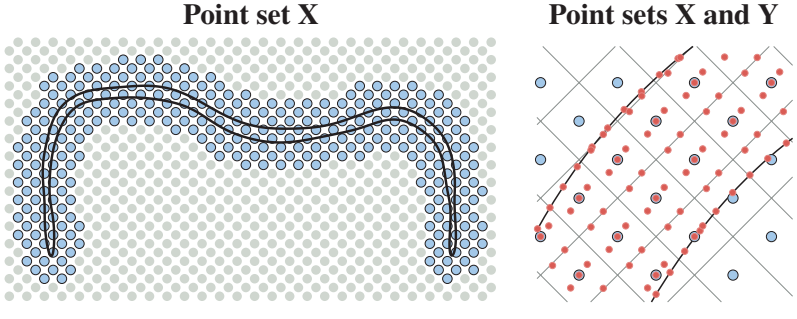

Figure 5.1. Left: a template point set is distributed over a box enclosing the boundary of the 2-dimensional diaphragm (black curve). Points more than half a stencil size away from the boundary (grey) are removed. The remaining points (blue) form the point set X. Right: A close-up onto a segment of the diaphragm, where blue points are from the point set X (unfitted to the boundary), and red points are from the evaluation point set Y (fitted to the boundary).

develop an unfitted RBF-FD method over an unfitted point set X (the steps are described in Section 3.3), and then discretized a stationary PDE (an elliptic model problem) as described in Section 4.1 by means of oversampling using a fitted point set Y. The unfitted point set X was constructed such that each stencil (local interpolant) had at least half of its support inside the computational domain, which was important for achieving a reasonable condition number

for the discretization matrices. Condition numbers when following the stencil support criterion were well behaved as $h \to 0$, and no other stabilization due to the extended point set was needed. Additional stabilizations are otherwise many times essential to use for other unfitted methods. We did not impose the Dirichlet boundary conditions strongly, but we instead used a weak approach through the oversampled discretization (see Section 4.1). A benefit that we numerically observed for several test cases was that when using a high-order polynomial basis to construct the local interpolation problems, the approximation error with the unfitted RBF-FD method was smaller compared with the fitted RBF-FD method. This was attributed to the shape of the stencils close to the boundary, which are less skewed in the unfitted setting compared with the fitted setting (see Figure 5.3). The developed method was then used in Paper

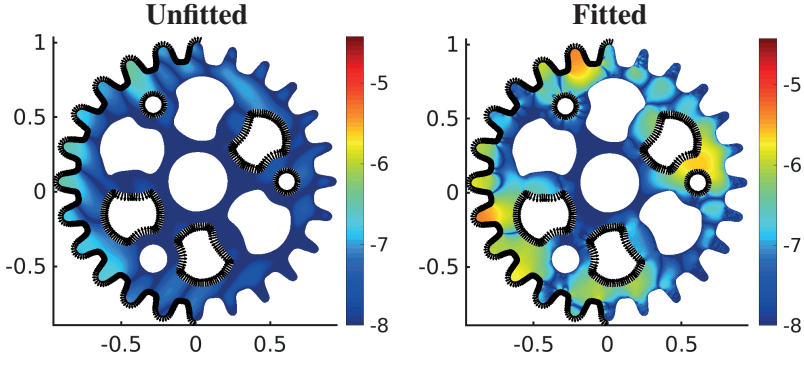

Figure 5.2. Spatial approximation error distribution in $\log_{10}$ scale, for a solution of the Poisson equation with mixed boundary conditions, when using two high-order oversampled RBF-FD methods. Black arrows correspond to locations where the Neumann boundary condition was imposed.

III to solve an elastic model over a two-dimensional slice of a thoracic diaphragm geometry obtained from a 3D computerized tomography (CT) scan, where the geometry is displayed in Figure 5.1.

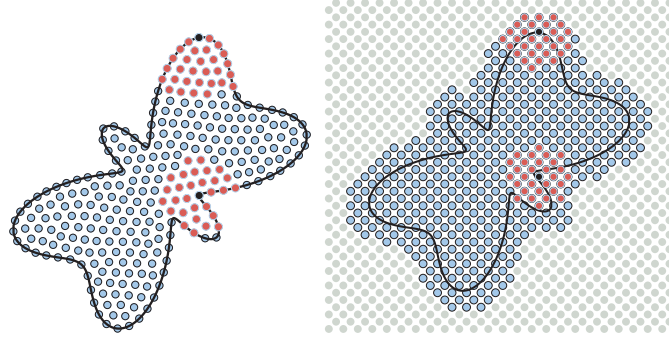

Figure 5.3. A conforming node set X with skewed stencils (left) and a non-conforming node set X with less skewed stencils (right).

6. Shock-stabilized radial basis function methods for solving time-dependent nonlinear conservation laws

Time-dependent PDE problems of type (2.2), where the flux F is nonlinear and does not contain any viscous forces, are difficult to solve numerically, as their exact solutions become discontinuous as $t \to \infty$. The discontinuities are also referred to as shocks. When solutions which include shocks are approximated by means of, at least locally continuous, cardinal basis functions, such as the ones defined in Section 3, then the approximation exhibits oscillations over the shock, see Figure 6.1. The oscillations do not vanish as $h \to 0$. This numerical effect is in the literature referred to as the Gibbs phenomenon [30]. To damp

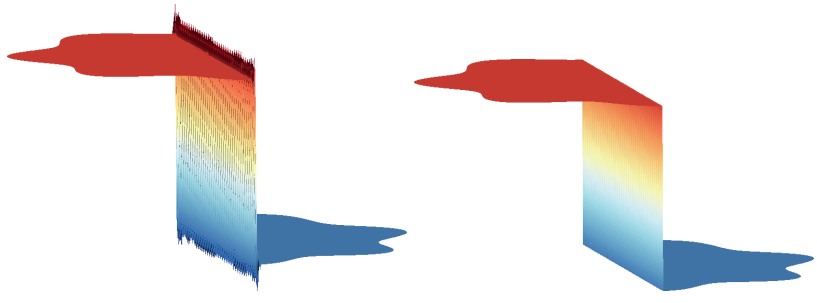

Figure 6.1. Numerical piecewise continuous approximation of a discontinuous function exhibiting the Gibbs phenomenon (left). A corresponding exact discontinuous function (right).

the oscillations across a shock, von Neumann and Richtmyer in 1950 [71] supplemented the PDE problem (2.2) with an artificial viscosity term. The PDE problem then became:

$$\partial_t u(y,t) = -\nabla \cdot F(u(y,t),t) + \nabla \cdot (\gamma \nabla u(y,t)), \tag{6.1}$$

with appropriate boundary conditions and initial conditions. In the limit $\gamma \to 0$, the solution of (6.1) converges to the exact solution of (2.2). When $\gamma > 0$ is fixed, then the solution of (6.1) is called a viscous solution. One of the possibilities to choose γ that makes the viscosity term to vanish as $h \to 0$ is $\gamma = \gamma_{\mathrm{UW}}$, where γ_{UW} is referred to as first-order viscosity parameter defined by:

$$\gamma_{\mathrm{UW}}(x_i,t_n) = \frac{1}{2} h_{\mathrm{loc}}(x_i) \sqrt{(F_1'(u(x_i,t_n),t_n))^2 + (F_2'(u(x_i,t_n),t_n))^2}. \tag{6.2}$$

Here $h_{\text{loc}}(x_i)$ is the minimum pairwise distance among the set of the 5 points closest to x_i. The h-dependence makes the artificial viscosity term vanish to 0 as $h \to 0$. The effect of the first-order artificial viscosity operator is that it diffuses the solution throughout the computational domain, and not only in the regions with shocks. While this is sufficient to stabilize the Gibbs phenomenon, it can lead to a loss of relevant waves in the numerical solution when h is fixed, for example a contact discontinuity or a rarefaction. A possibility to localize the action of the viscosity term only to regions that contain shocks, is to modify γ according to a residual-based artificial viscosity (RV) term [53]. In each time step, and at each point $x_i \in X$, γ is:

$$\begin{aligned} \gamma(x_i, t_{n+1}) &= \min\left(\gamma_{\text{RV}}(x_i, t_n), \gamma_{\text{UW}}(x_i, t_n)\right), \quad n = 2, 3, \ldots \\ \gamma(x_i, t_{n+1}) &= \gamma_{\text{UW}}(x_i, t_n), \quad n = 1. \end{aligned} \tag{6.3}$$

Here γ_{UW} is already defined in (6.2). The coefficient γ_{RV} is defined by:

$$\gamma_{\text{RV}}(x_i, t_{n+1}) = C_{\text{RV}}\, h_{\text{loc}}^2(x_i) \max_{y_j \in K_i} |R(y_j, t_n)| \frac{1}{n(x_i, t_n)}, \tag{6.4}$$

where $n(x_i, t_n)$ is a normalization term, C_{RV} is a user-defined $\mathcal{O}(1)$ constant, K_i is a Voronoi cell centered around x_i, and $R(y_j, t_n)$ is the PDE residual evaluated at $y_j \in Y$. The PDE residual is a shock indicator: the residual values are expected to be very large in the regions of shocks, where the numerical solution has an overshoot, but very small in the regions where the solution is smooth. The viscosity coefficient γ from (6.3) is then set to a very small number in the smooth regions, and to γ_{UW} in the regions with shocks, which is desired. RV has its roots in the finite element community. At first, it was

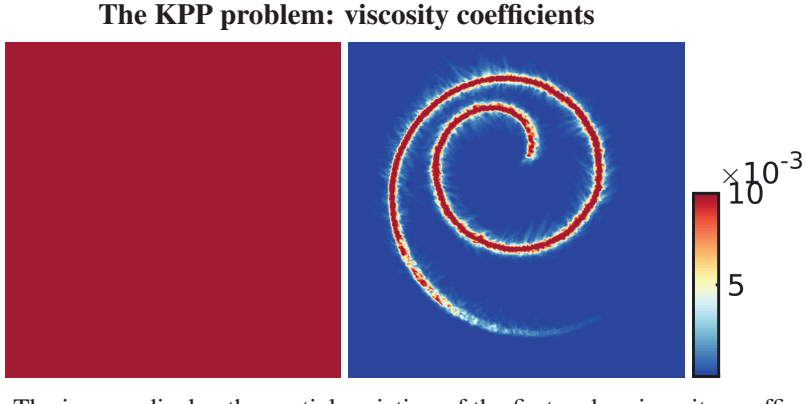

Figure 6.2. The images display the spatial variation of the first-order viscosity coefficient γ_{UW} (left), and the viscosity coefficient $\gamma = \min(\gamma_{\text{UW}}, \gamma_{\text{RV}})$ (right) when solving the Kurganov-Petrova-Popov problem.

used to improve the stabilization effects of the streamline diffusion stabilization method in [36]. In [53] the streamline diffusion terms were removed and

only the RV term was kept. That provided a sufficient stabilization effect in practice [54]. In [53] the RV stabilization framework was also proven to stabilize numerical solutions with shocks, when the numerical solution comes from a finite element space, and where the numerical solution is advanced in time by an implicit time stepping algorithm.

In Paper V we stabilize the RBF-FD solutions to nonlinear hyperbolic time-dependent problems by using the RV term to localize the effect of the artificial viscosity term to regions with shocks. We solve a number of benchmark problems, where the governing PDEs are: Burger's equation, the Kurganov-Petrova-Popov (KPP) problem, and the Euler system of equations. An example of the spatial variation of the viscosity coefficients γ_{UW} (6.2) and γ (6.3) are given in Figure 6.2. The displayed coefficients correspond to the numerical solution of the KPP problem from Figure 6.3.

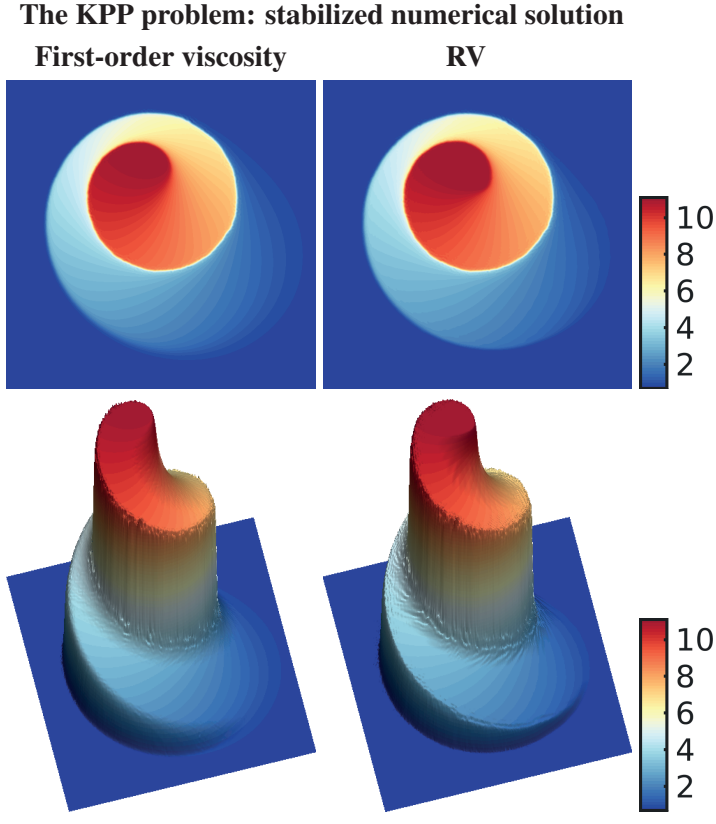

Figure 6.3. A numerical solution to the Kurganov-Petrova-Popov problem from a top perspective (first row) and a side perspective (second row), when two different shock stabilizations are added to the oversampled RBF-FD discretization.

7. Towards the simulation of a thoracic diaphragm

The thoracic diaphragm is the muscle that drives the respiratory system of a human being. The action of the diaphragm affects the volume of the thorax cavity, such that the lungs can inflate and deflate, enabling a human to breathe. The diaphragm geometry is a thin volume which is also highly non-convex (see Figure 7.1). One of the goals of the present thesis is to develop compu-

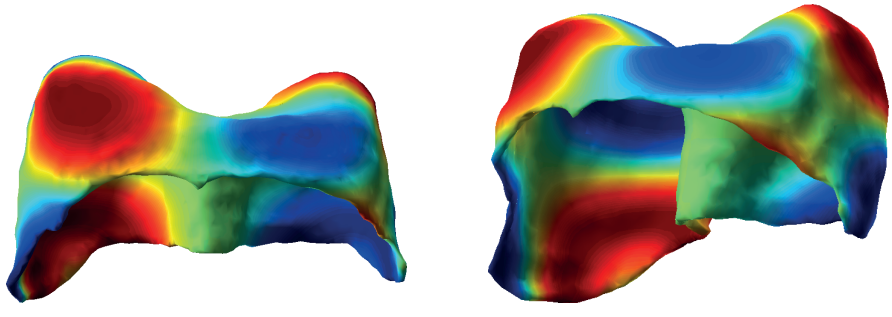

Figure 7.1. A reconstructed diaphragm geometry displayed from two different angles. The colors over the surface represent a sinusoidal scalar field.

tational methods that can solve a mathematical (PDE) model defined over the diaphragm geometry. A wider context is to enable medical researchers to perform computational studies on ventilator induced diaphragm disease (VIDD) [48]. VIDD can many times occur as a secondary disease while a patient is mechanically ventilated in an intensive care unit due to some primary disease, such as for example an infection with covid-19. It is important that computational studies are performed using methods that are robust and accurate, but the methods also have to be computationally inexpensive, so that the researchers can continuously modify physiological parameters of the model and quickly obtain a new computational result. High-order methods are a resource for improving the computational cost. Their benefit is that they give numerical solutions with a given accuracy for a smaller computational cost, compared to low-order methods. A requirement for high-order methods to be applicable is, however, that the PDE model has sufficiently smooth data such as: the forcing data, the boundary condition data and the boundary of the computational domain. Most common problems in solid mechanics do not have data and boundary conditions with a sufficient smoothness. For example, a linear

elasticity problem in displacement form:

$$-\mu\nabla^2 u-(\lambda+\mu)\nabla(\nabla\cdot u)=f \text{ on } \Omega, \tag{7.1}$$

is equipped by displacement boundary conditions and traction boundary conditions, imposed on two disjoint parts of $\partial\Omega$:

$$\begin{aligned} u &= g \text{ on } \partial\Omega_0, \\ \left(\left[\lambda\left(\nabla\cdot u\right)I+\mu\left(\left(\nabla u\right)^T+\nabla u\right)\right]\cdot n\right) &= h \text{ on } \partial\Omega_1. \end{aligned} \tag{7.2}$$

Here $\partial\Omega=\partial\Omega_0\cup\partial\Omega_1$, u is a vector of displacements, n is the outwards normal from Ω, the coefficients λ,μ are the elastic Lamé parameters, and I is an identity matrix. An equivalent, more compact, form of the mixed boundary conditions (7.2) is:

$$u\,\kappa_0+\left(\left[\lambda\left(\nabla\cdot u\right)I+\mu\left(\left(\nabla u\right)^T+\nabla u\right)\right]\cdot n\right)\kappa_1 = g\,\kappa_0+h\,\kappa_1 \text{ on } \partial\Omega,$$

where κ_0,κ_1 are discontinuous coefficients such that $\kappa_0=1$ on $\partial\Omega_0$ and $\kappa_0=0$ on $\partial\Omega_1$, while $\kappa_1=0$ on $\partial\Omega_0$ and $\kappa_1=1$ on $\partial\Omega_1$. If we construct the coefficients κ_0 and κ_1 such that they have a smooth transition between 0 and 1, then we can leverage high-order convergence to improve the computational cost. Here we also have to assure that the boundary functions g and h are sufficiently smooth at each point of $\partial\Omega_0$ and $\partial\Omega_1$, and that the forcing function f from (7.1) is smooth over the whole Ω, and also that the representation of $\partial\Omega$ is smooth. Smoothing of data can introduce modeling errors, however, in the diaphragm case, the real problem already entails smooth data, which additionally justifies smoothing of the data used in the computational model.

In Paper III we used an unfitted RBF-FD method to solve a linear elastic problem on a two-dimensional slice of the diaphragm (Figure 5.1). The slice was extracted from a real 3D CT scan. We developed a framework by which we constructed smooth κ_0 and κ_1, smoothed the boundary data functions f and g, smoothed the boundary of the 2D diaphragm geometry, solved two model test cases, and observed high-order convergence of the numerical solution to a reference solution obtained by the finite element method.

8. Final discussion

Throughout the present thesis, we use PDE discretizations that utilize an oversampled approach. This provides control over the stability properties of the RBF methods that are applied to stationary PDE problems and time-dependent PDE problems. Admittedly, controlling the stability properties through oversampling is suboptimal, as a large number of evaluation points have to be employed to make the solutions stable, especially for time-dependent (nearly) hyperbolic PDE problems. Using quadrature rules exact for integrating cardinal basis functions, instead of employing oversampling, would have been much better from a stability perspective, as the stability estimates would never entail a spurious integration error term. The latter is a clear advantage of finite element methods for example. However, a mesh is required to construct such quadrature rules which is — in the meshfree community — many times avoided to keep the method implementation simple. In this sense, the oversampled type of discretizations is an excellent middle ground between the collocation framework, where it is not possible to control the stability properties without adding additional stabilization terms, and the fully variational framework employing quadrature rules. Oversampled discretizations also allow a theoretical insight into the stability properties by employing a variational point of view. The variational point of view, for example, enabled us to investigate why RBF-FD methods are not stable by construction when solving a linear time-dependent hyperbolic PDE with a smooth initial condition. The oversampling approach also made it possible to develop an unfitted RBF-FD method with significant simplifications of the node placing over the computational domain and an improved approximation error near the boundary of the domain. On the other hand, it is vital to acknowledge that collocated RBF discretizations have been successfully used for many applications in the last decades. Collocation methods are also computationally cheaper, especially when they are used for time-dependent PDE problems. To conclude, oversampled RBF methods link to a theoretical framework with controllable stability properties, are therefore easier to motivate in terms of their relevance to the scientific computing community, and can perform better compared with the basic collocation methods when discretizing PDEs that entail derivative-type boundary conditions, a scenario faced many times in solid mechanics and fluid mechanics.

Acknowledgments

I am deeply grateful to my advisor Prof. Elisabeth Larsson. Thank you, Elisabeth, for introducing me to the subject, for always making yourself available to have discussions with me, for trying to see potential in my research ideas and for setting an example for how to work hard.

I would also like to thank my secondary advisors Dr. Nicola Cacciani, MD, and Assoc. Prof. Pierre-Frédéric Villard. Nicola and Pierre, thank you for all the exciting discussions we have had, for all the work that we have done together, and for always creating a cheerful working atmosphere whenever we met.

Whenever I knocked on the office door of Assoc. Prof. Murtazo Nazarov, he always warmly welcomed me and took the time to have discussions about various topics in numerical analysis with me, even if he was busy doing other things. Murtazo, I had a great time learning from you and staying in your company.

It was during the beginning of my PhD studies that I met Assoc. Prof. Víctor Bayona at one of the conferences. I find it wonderful that we have been managing to keep in touch to this day, even if Uppsala is far away from Madrid. Thank you, Víctor, for sharing your knowledge with me.

Many thanks to my office mates, Gustav Ludvigsson, and Sonja Mathias. Gustav, thank you for showing me how to lift gym weights correctly and for having many discussions about finite element methods with me. Sonja, thank you for saving my life when I, one day, nearly choked myself chewing on a banana-chocolate protein bar.

To all PhD students and graduates whom I met at the Division of Scientific Computing: I feel privileged to have had an opportunity to learn from you.

To my dear and loving Eva. Thank you for standing by my side. You are my essential boundary condition, making my life well-posed. I am also grateful to our dear Sever, for bringing so much happiness to our lives.

Sammanfattning på svenska

Partiella differentialekvationer (PDE) beskriver komplexa fenomen i verkligheten såsom väderförändringar, deformation av olika objekt, prisutvecklingen på finansmarknaden och den ömsesidiga påverkan mellan vätskor och solida föremål. Lösningarna till PDE:er används ofta för att öka förståelsen av dessa fenomen och även som ett verktyg för att göra tekniska förbättringar av konsumentprodukter. I den här avhandlingen, utvecklar vi numeriska metoder för att lösa PDE:er med hjälp av datorer. Fokus ligger på radiella basfunktionsmetoder (RBF) som uppskattas för sin höga noggrannhet och för att de är lätta att implementera i högre dimensioner, men som ibland kan ha problem med den numeriska stabiliteten. För att kringgå stabilitetsproblemen använder vi ett översamplat ramverk för att diskretisera PDE:er i motsats till det mer vanligen använda kollokationsramverket. Genom hela avhandlingen använder vi huvudsakligen den RBF-genererade finita differensmetoden (RBF-FD), men vi använder också en RBF-enhetsuppdelningsmetod (RBF-PUM) och Kansas globala RBF-metod i en del av avhandlingen. De två första metoderna är lokala i den meningen att de underliggande diskretiseringsmatriserna är glesa, medan den tredje metoden är global, vilket leder till fyllda diskretiseringsmatriser. I Paper I förbättrar vi stabilitetsegenskaperna för RBF-FD-metoden genom översampling vid lösning av ett elliptiskt modellproblem med randvillkor av derivatatyp samt genomför en teoretisk analys. I Paper II utvecklar vi en oanpassad RBF-FD-metod och förenklar därmed hanteringen av komplexa beräkningsområden genom att släppa kravet på att noduppsättningen måste ansluta till randen av området. Vi tar de första stegen mot en simulering av diafragman i Paper III, där vi använder en oanpassad RBF-FD-metod för att lösa en linjär elastisk PDE och använder datautjämning för att kunna åtnjuta högre ordningens konvergens i den numeriska lösningen. I Paper IV utforskar vi stabilitetsegenskaperna hos RBF-FD-metoden, Kansas metod och RBF-PUM när de tillämpas på en linjär tidsberoende hyperbolisk PDE. Vi finner att Kansas metod och RBF-PUM kan bli stabila under tillräcklig översampling av ekvationssystemet. Å andra sidan förhindrar den otillräckliga kontinuiteten hos den numeriska lösningen att RBF-FD-metoden blir stabil i tiden, oavsett översampling. I Paper V använder vi ett residualviskositetsstabiliseringsramverk för att lokalt stabilisera Gibbs fenomen som finns i RBF-FD-lösningarna till olinjära tidsberoende konserveringslagar med stötar såsom kompressibla Eulers ekvationer.

Genom hela avhandlingen använder vi PDE-diskretiseringar som använder ett översamplat tillvägagångssätt. Detta ger kontroll över stabilitetsegenskaperna hos RBF-metoderna, som tillämpas på stationära PDE-problem och

tidsberoende PDE-problem. Visserligen är det suboptimalt att kontrollera stabilitetsegenskaperna genom översampling, eftersom många evalueringspunkter måste användas för att göra lösningarna stabila, särskilt för tidsberoende (nästan) hyperboliska PDE-problem. Att använda exakt integration istället för översampling skulle ha varit mycket bättre ur ett stabilitetsperspektiv, eftersom stabilitetsuppskattningarna inte skulle innehålla en integrationsfelterm. Det senare är en tydlig fördel med till exempel finita elementmetoder. Emellertid krävs ett nät för att konstruera en exakt integration, vilket—bland forskare som arbetar med nätfria metoder—många gånger undviks för att göra metodimplementeringen enkel. I det avseendet är den översamplade typen av diskretiseringar en utmärkt kompromiss mellan kollokationssramverket, där det inte är möjligt att kontrollera stabilitetsegenskaperna utan att lägga till ytterligare stabiliseringsvillkor, och variationsramverket med exakt integration. Översamplade diskretiseringar tillåter också en teoretisk insikt i stabilitetsegenskaperna genom att anlägga ett variationsperspektiv. Variationsperspektivet gjorde det till exempel möjligt för oss att undersöka varför RBF-FD-metoder inte är stabila genom sin konstruktion när man löser en linjär tidsberoende hyperbolisk PDE med ett glatt initialtillstånd. Översamplingsmetoden gjorde det också möjligt att utveckla en oanpassad RBF-FD-metod med betydande förenklingar av nodpunkternas placering över beräkningsområdet och ett förbättrat approximationsfel nära områdets rand. Å andra sidan är det viktigt att understryka att kollokerade RBF-diskretiseringar har använts framgångsrikt för många tillämpningsproblem under de senaste decennierna. Kollokationsmetoder är också beräkningsmässigt billigare, speciellt när de används för tidsberoende PDE-problem. Sammanfattningsvis, översamplade RBF-metoder är kopplade till ett teoretiskt ramverk med kontrollerbara stabilitetsegenskaper och är därför lättare att motivera när det gäller deras relevans för det beräkningsvetenskapliga området och kan prestera bättre jämfört med de grundläggande kollokationsmetoderna vid diskretisering av PDE:er som har randvillkor av derivatatyp, ett scenario som är vanligt inom solidmekanik och fluidmekanik.

References

[1] Josefin Ahlkrona and Victor Shcherbakov. A meshfree approach to non-Newtonian free surface ice flow: application to the Haut Glacier d'Arolla. *J. Comput. Phys.*, 330:633–649, 2017.

[2] Ivo Babuška and Jens Markus Melenk. The partition of unity method. *Internat. J. Numer. Methods Engrg.*, 40(4):727–758, 1997.

[3] Gregory A. Barnett. *A Robust RBF-FD Formulation based on Polyharmonic Splines and Polynomials*. Ph.D. thesis, University of Colorado at Boulder, Dept. of Applied Mathematics, Boulder, CO, USA, 2015.

[4] Simon Barthelmé and Konstantin Usevich. Spectral properties of kernel matrices in the flat limit. *SIAM J. Matrix Anal. Appl.*, 42(1):17–57, 2021.

[5] Víctor Bayona. An insight into RBF-FD approximations augmented with polynomials. *Comput. Math. Appl.*, 77:2337–2353, 2019.

[6] Víctor Bayona, N. Flyer, G. M. Lucas, and A. J. G. Baumgaertner. A 3-d rbf-fd solver for modeling the atmospheric global electric circuit with topography (gec-rbffd v1.0). *Geoscientific Model Development*, 8(10):3007–3020, 2015.

[7] Víctor Bayona, Natasha Flyer, and Bengt Fornberg. On the role of polynomials in RBF-FD approximations: III. Behavior near domain boundaries. *J. Comput. Phys.*, 380:378–399, 2019.

[8] Víctor Bayona, Natasha Flyer, Bengt Fornberg, and Gregory A. Barnett. On the role of polynomials in RBF-FD approximations: II. Numerical solution of elliptic PDEs. *J. Comput. Phys.*, 332:257–273, 2017.

[9] Víctor Bayona, Mario Sánchez-Sanz, Eduardo Fernández-Tarrazo, and Manuel Kindelan. Micro-combustion modelling with RBF-FD: a high-order meshfree method for reactive flows in complex geometries. *Appl. Math. Model.*, 94:635–655, 2021.

[10] Susanne C. Brenner and L. Ridgway Scott. *The mathematical theory of finite element methods*, volume 15 of *Texts in Applied Mathematics*. Springer, New York, third edition, 2008.

[11] M. D. Buhmann. *Radial basis functions: theory and implementations*, volume 12 of *Cambridge Monographs on Applied and Computational Mathematics*. Cambridge University Press, Cambridge, 2003.

[12] Erik Burman and Peter Hansbo. Fictitious domain finite element methods using cut elements: I. A stabilized Lagrange multiplier method. *Comput. Methods Appl. Mech. Engrg.*, 199(41-44):2680–2686, 2010.

[13] Gong Cheng and Victor Shcherbakov. Anisotropic radial basis function methods for continental size ice sheet simulations. *J. Comput. Phys.*, 372:161–177, 2018.

[14] Ka Chun Cheung, Leevan Ling, and Robert Schaback. H^2-convergence of least-squares kernel collocation methods. *SIAM J. Numer. Anal.*, 56(1):614–633, 2018.

[15] Tobin A. Driscoll and Bengt Fornberg. Interpolation in the limit of increasingly flat radial basis functions. volume 43, pages 413–422. 2002. Radial basis functions and partial differential equations.
[16] Gregory E. Fasshauer. Solving differential equations with radial basis functions: multilevel methods and smoothing. volume 11, pages 139–159. 1999. Radial basis functions and their applications.
[17] Gregory E. Fasshauer. *Meshfree approximation methods with MATLAB*, volume 6 of *Interdisciplinary Mathematical Sciences*. World Scientific Publishing Co. Pte. Ltd., Hackensack, NJ, 2007. With 1 CD-ROM (Windows, Macintosh and UNIX).
[18] Natasha Flyer, Gregory A. Barnett, and Louis J. Wicker. Enhancing finite differences with radial basis functions: experiments on the Navier-Stokes equations. *J. Comput. Phys.*, 316:39–62, 2016.
[19] Natasha Flyer, Bengt Fornberg, Víctor Bayona, and Gregory A. Barnett. On the role of polynomials in RBF-FD approximations: I. Interpolation and accuracy. *J. Comput. Phys.*, 321:21–38, 2016.
[20] Natasha Flyer, Erik Lehto, Sébastien Blaise, Grady B. Wright, and Amik St-Cyr. A guide to RBF-generated finite differences for nonlinear transport: shallow water simulations on a sphere. *J. Comput. Phys.*, 231(11):4078–4095, 2012.
[21] Bengt Fornberg and Natasha Flyer. *A primer on radial basis functions with applications to the geosciences*, volume 87 of *CBMS-NSF Regional Conference Series in Applied Mathematics*. Society for Industrial and Applied Mathematics (SIAM), Philadelphia, PA, 2015.
[22] Bengt Fornberg, Elisabeth Larsson, and Natasha Flyer. Stable computations with Gaussian radial basis functions. *SIAM J. Sci. Comput.*, 33(2):869–892, 2011.
[23] Bengt Fornberg and Erik Lehto. Stabilization of RBF-generated finite difference methods for convective PDEs. *J. Comput. Phys.*, 230(6):2270–2285, 2011.
[24] Bengt Fornberg and Cécile Piret. A stable algorithm for flat radial basis functions on a sphere. *SIAM J. Sci. Comput.*, 30(1):60–80, 2007/08.
[25] Bengt Fornberg and G. Wright. Stable computation of multiquadric interpolants for all values of the shape parameter. *Comput. Math. Appl.*, 48(5-6):853–867, 2004.
[26] Bengt Fornberg, G. Wright, and Elisabeth Larsson. Some observations regarding interpolants in the limit of flat radial basis functions. *Comput. Math. Appl.*, 47(1):37–55, 2004.
[27] Carsten Franke and Robert Schaback. Convergence order estimates of meshless collocation methods using radial basis functions. *Adv. Comput. Math.*, 8(4):381–399, 1998.
[28] Carsten Franke and Robert Schaback. Solving partial differential equations by collocation using radial basis functions. *Appl. Math. Comput.*, 93(1):73–82, 1998.
[29] G. Garmanjani, R. Cavoretto, and M. Esmaeilbeigi. A RBF partition of unity collocation method based on finite difference for initial-boundary value problems. *Comput. Math. Appl.*, 75(11):4066–4090, 2018.
[30] J. Willard Gibbs. Fourier's series. *Nature*, 195, 1899.
[31] Peter Hansbo, Mats G. Larson, and Sara Zahedi. A cut finite element method

for a Stokes interface problem. *Appl. Numer. Math.*, 85:90–114, 2014.
[32] Rolland L. Hardy. Multiquadric equations of topography and other irregular surfaces. *Journal of Geophysical Research (1896-1977)*, 76(8):1905–1915, 1971.
[33] Vanja Hatić, Boštjan Mavrič, Nejc Košnik, and Božidar Šarler. Simulation of direct chill casting under the influence of a low-frequency electromagnetic field. *Appl. Math. Model.*, 54:170–188, 2018.
[34] Armin Iske. On the approximation order and numerical stability of local Lagrange interpolation by polyharmonic splines. In *Modern developments in multivariate approximation*, volume 145 of *Internat. Ser. Numer. Math.*, pages 153–165. Birkhäuser, Basel, 2003.
[35] Mozhgan Jabalameli and Davoud Mirzaei. A weak-form RBF-generated finite difference method. *Comput. Math. Appl.*, 79(9):2624–2643, 2020.
[36] Claes Johnson, Anders Szepessy, and Peter Hansbo. On the convergence of shock-capturing streamline diffusion finite element methods for hyperbolic conservation laws. *Math. Comp.*, 54(189):107–129, 1990.
[37] Edward J. Kansa. Application of Hardy's multiquadric interpolation to hydrodynamics. NASA STI/Recon Technical Report N, October 1985.
[38] Edward J. Kansa. Multiquadrics—a scattered data approximation scheme with applications to computational fluid-dynamics. I. Surface approximations and partial derivative estimates. *Comput. Math. Appl.*, 19(8-9):127–145, 1990.
[39] Edward J. Kansa. Multiquadrics—a scattered data approximation scheme with applications to computational fluid-dynamics. II. Solutions to parabolic, hyperbolic and elliptic partial differential equations. *Comput. Math. Appl.*, 19(8-9):147–161, 1990.
[40] Katharina Kormann and Elisabeth Larsson. A Galerkin radial basis function method for the Schrödinger equation. *SIAM J. Sci. Comput.*, 35(6):A2832–A2855, 2013.
[41] Katharina Kormann, Caroline Lasser, and Anna Yurova. Stable interpolation with isotropic and anisotropic gaussians using hermite generating function. *SIAM J. Sci. Comput.*, 41(6):A3839–A3859, 2019.
[42] Ting-On Kwok and Leevan Ling. On convergence of a least-squares Kansa's method for the modified Helmholtz equations. *Adv. Appl. Math. Mech.*, 1(3):367–382, 2009.
[43] Elisabeth Larsson and Bengt Fornberg. Theoretical and computational aspects of multivariate interpolation with increasingly flat radial basis functions. *Comput. Math. Appl.*, 49(1):103–130, 2005.
[44] Elisabeth Larsson, Erik Lehto, Alfa Heryudono, and Bengt Fornberg. Stable computation of differentiation matrices and scattered node stencils based on Gaussian radial basis functions. *SIAM J. Sci. Comput.*, 35(4):A2096–A2119, 2013.
[45] Elisabeth Larsson, Victor Shcherbakov, and Alfa Heryudono. A least squares radial basis function partition of unity method for solving PDEs. *SIAM J. Sci. Comput.*, 39(6):A2538–A2563, 2017.
[46] Damiana Lazzaro and Laura B. Montefusco. Radial basis functions for the multivariate interpolation of large scattered data sets. In *Proceedings of the 9th International Congress on Computational and Applied Mathematics (Leuven,*

2000), volume 140, pages 521–536, 2002.

[47] Cheng-Feng Lee, Leevan Ling, and Robert Schaback. On convergent numerical algorithms for unsymmetric collocation. *Adv. Comput. Math.*, 30(4):339–354, 2009.

[48] Monica Llano-Diez, Guillaume Renaud, Magnus Andersson, Humberto Gonzales Marrero, Nicola Cacciani, Henrik Engquist, Rebeca Corpeño, Konstantin Artemenko, Jonas Bergquist, and Lars Larsson. Intensive care unit muscle wasting : mechanisms and intervention strategies. *Critical Care*, 16:R209, 2012.

[49] Nathaniel H. Mathews, Natasha Flyer, and Sarah E. Gibson. Solving 3d magnetohydrostatics with rbf-fd: Applications to the solar corona, 2021.

[50] Charles A. Micchelli. Interpolation of scattered data: distance matrices and conditionally positive definite functions. *Constr. Approx.*, 2(1):11–22, 1986.

[51] Slobodan Milovanović and Lina von Sydow. A high order method for pricing of financial derivatives using radial basis function generated finite differences. *Math. Comput. Simulation*, 174:205–217, 2020.

[52] Francis J. Narcowich and Joseph D. Ward. Norms of inverses and condition numbers for matrices associated with scattered data. *J. Approx. Theory*, 64(1):69–94, 1991.

[53] Murtazo Nazarov. Convergence of a residual based artificial viscosity finite element method. *Comput. Math. Appl.*, 65(4):616–626, 2013.

[54] Murtazo Nazarov and Johan Hoffman. Residual-based artificial viscosity for simulation of turbulent compressible flow using adaptive finite element methods. *Internat. J. Numer. Methods Fluids*, 71(3):339–357, 2013.

[55] Charles S. Peskin. Flow patterns around heart valves. In *Proceedings of the Third International Conference on Numerical Methods in Fluid Mechanics (Univ. Paris VI and XI, Paris, 1972), Vol. II*, pages 214–221. Lecture Notes in Phys., Vol. 19, 1973.

[56] Ulrika Pettersson, Elisabeth Larsson, Gunnar Marcusson, and Jonas Persson. Improved radial basis function methods for multi-dimensional option pricing. *J. Comput. Appl. Math.*, 222(1):82–93, 2008.

[57] Robert Schaback. Error estimates and condition numbers for radial basis function interpolation. *Adv. Comput. Math.*, 3(3):251–264, 1995.

[58] Robert Schaback. Convergence of unsymmetric kernel-based meshless collocation methods. *SIAM J. Numer. Anal.*, 45(1):333–351, 2007.

[59] Varun Shankar. The overlapped radial basis function-finite difference (RBF-FD) method: a generalization of RBF-FD. *J. Comput. Phys.*, 342:211–228, 2017.

[60] Victor Shcherbakov. Radial basis function partition of unity operator splitting method for pricing multi-asset American options. *BIT*, 56(4):1401–1423, 2016.

[61] Donald Shepard. A two-dimensional interpolation function for irregularly-spaced data. In *Proceedings of the 1968 23rd ACM National Conference*, ACM '68, page 517–524, New York, NY, USA, 1968. Association for Computing Machinery.

[62] Stanislav Simonenko, Víctor Bayona, and Manuel Kindelan. Optimal shape parameter for the solution of elastostatic problems with the RBF method. *J. Engrg. Math.*, 85:115–129, 2014.

[63] Jure Slak and Gregor Kosec. Adaptive radial basis function-generated finite

differences method for contact problems. *Internat. J. Numer. Methods Engrg.*, 119(7):661–686, 2019.
[64] Simon Sticko, Gustav Ludvigsson, and Gunilla Kreiss. High-order cut finite elements for the elastic wave equation. *Adv. Comput. Math.*, 46(3):Paper No. 45, 28, 2020.
[65] Vidar Stiernström, Lukas Lundgren, Murtazo Nazarov, and Ken Mattsson. A residual-based artificial viscosity finite difference method for scalar conservation laws. *J. Comput. Phys.*, 430:110100, 2021.
[66] Andrei I. Tolstykh. On using RBF-based differencing formulas for unstructured and mixed structured-unstructured grid calculations. In *Proceedings of the 16th IMACS World Congress on Scientific Computation, Applied Mathematics and Simulation*, Lausanne, Switzerland, 2002.
[67] Andrei I. Tolstykh and D. A. Shirobokov. On using radial basis functions in a "finite difference mode" with applications to elasticity problems. *Comput. Mech.*, 33(1):68–79, 2003.
[68] Igor Tominec. Rectangular and square RBF-FD matrices in MATLAB. `https://github.com/IgorTo/rbf-fd`, 2021.
[69] Siraj ul Islam, Rrobert Vertnik, and Božidar Šarler. Local radial basis function collocation method along with explicit time stepping for hyperbolic partial differential equations. *Appl. Numer. Math.*, 67:136–151, 2013.
[70] Robert Vertnik and Božidar Šarler. Simulation of continuous casting of steel by a meshless technique. *International Journal of Cast Metals Research*, 22(1-4):311–313, 2009.
[71] John Von Neumann and Robert D. Richtmyer. A method for the numerical calculation of hydrodynamic shocks. *J. Appl. Phys.*, 21:232–237, 1950.
[72] Holger Wendland. Piecewise polynomial, positive definite and compactly supported radial functions of minimal degree. *Adv. Comput. Math.*, 4(4):389–396, 1995.
[73] Holger Wendland. Meshless Galerkin methods using radial basis functions. *Math. Comp.*, 68(228):1521–1531, 1999.
[74] Holger Wendland. Fast evaluation of radial basis functions: methods based on partition of unity. In *Approximation theory, X (St. Louis, MO, 2001)*, Innov. Appl. Math., pages 473–483. Vanderbilt Univ. Press, Nashville, TN, 2002.
[75] Grady B. Wright, Natasha Flyer, and David A. Yuen. A hybrid radial basis function-pseudospectral method for thermal convection in a 3-d spherical shell. *Geochemistry Geophysics Geosystems*, 11, 2010.
[76] Grady B. Wright and Bengt Fornberg. Stable computations with flat radial basis functions using vector-valued rational approximations. *J. Comput. Phys.*, 331:137–156, 2017.
[77] G Yang, DM Causon, DM Ingram, R Saunders, and P Battent. A cartesian cut cell method for compressible flows part a: Static body problems. *The Aeronautical Journal*, 101(1002):47–56, 1997.
[78] Hui Zheng, Chuanzeng Zhang, Yuesheng Wang, Jan Sladek, and Vladimir Sladek. A meshfree local RBF collocation method for anti-plane transverse elastic wave propagation analysis in 2D phononic crystals. *J. Comput. Phys.*, 305:997–1014, 2016.

Acta Universitatis Upsaliensis

Digital Comprehensive Summaries of Uppsala Dissertations from the Faculty of Science and Technology 2142

Editor: The Dean of the Faculty of Science and Technology

A doctoral dissertation from the Faculty of Science and Technology, Uppsala University, is usually a summary of a number of papers. A few copies of the complete dissertation are kept at major Swedish research libraries, while the summary alone is distributed internationally through the series Digital Comprehensive Summaries of Uppsala Dissertations from the Faculty of Science and Technology. (Prior to January, 2005, the series was published under the title "Comprehensive Summaries of Uppsala Dissertations from the Faculty of Science and Technology".)

Distribution: publications.uu.se
urn:nbn:se:uu:diva-472096

ACTA
UNIVERSITATIS
UPSALIENSIS
UPPSALA
2022